Supporting Information for:

Sodium-Coupled Electron Transfer Reactivity of Metal-Organic Frameworks Containing Titanium Clusters: The Importance of Cations in Redox Chemistry

Caroline T. Saouma,[‡,±,∞] Chih-Chin Tsou,[‡,δ,∞] Sarah R. Richard,[‡] Rob Ameloot,[ℓ] Frederik Vermoortele,[ℓ] Simon Smolders,[ℓ] Bart Bueken,[ℓ] Antonio DiPasquale,[⊥] Werner Kaminsky,[‡] Carolyn N. Valdez,[‡,δ] Dirk E. De Vos,*[,ℓ] James M. Mayer*[,‡,δ]

[∞] C.T.S. and C.-C. T. contributed equally to the manuscript.

[‡] Department of Chemistry, University of Washington, Box 351700, Seattle, Washington 98195-1700, U.S.A.

[ℓ] Centre for Surface Chemistry and Catalysis, KU Leuven – University of Leuven, Celestijnenlaan 200F p.o. box 2461, 3001 Leuven, Belgium, dirk.devos@kuleuven.be

[±] Department of Chemistry, University of Utah, 315 S 1400 E, Room 2020, Salt Lake City, UT 84102-0850, caroline.saouma@utah.edu

[δ] Department of Chemistry, Yale University, P.O. Box 208107, New Haven, CT 06520-8107, james.mayer@yale.edu

[⊥] Department of Chemistry, University of California, Latimer Hall, Berkeley, CA 94720

Table of Contents

A. General Considerations

Unless noted, all manipulations were carried out using standard Schlenk or glove-box techniques under a dinitrogen atmosphere. Glassware was oven-dried for 24 h prior to use. Celite and molecular sieves were dried by heating to 300 °C under vacuum for 24 h. Unless otherwise noted, solvents were deoxygenated and dried by sparging with Ar followed by passage through Grubbs-style columns filled with activated alumina.[1] Acetonitrile was purchased from Burdick and Jackson® (< 5ppm low-water brand) and stored in an Ar pressurized stainless steel drum plumbed directly into a glove-box. Isopropanol was dried by refluxing over Mg turnings for 12 h and distilled under N_2. All glove-box solvents were stored over activated 3 Å molecular sieves. Deuterated solvents were purchased from Cambridge Isotopes Laboratories, Inc. and were degassed and stored over activated 3 Å molecular sieves prior to use. d_3-MeCN was dried over CaH_2 and vacuum transferred prior to storage over sieves. Methanol was degassed and stored over activated 3 Å molecular sieves. d_8-THF was dried over sodium and benzophenone and then vacuum-transferred to a N_2-filled flask. d_3-MeCN was dried over $KMnO_4$, followed by a vacuum-transfer into a flask containing CaH_2. Deuterium solvents were not stored over molecular sieves (MS) due to a possible contamination of Na^+/K^+ ion in 4 Å MS (Na_2O•Al_2O_3•$2SiO_2$) and 3 Å MS ($2/3K_2O$•$1/3Na_2O$•Al_2O_3• 2 SiO_2). Elemental Analyses were performed at Complete Analysis Laboratories Inc. (Parsippany, NJ).

Reagents were purchased from Aldrich and unless noted, used without further purification. $CoCp^*_2$ and $CrCp^*_2$ were purified by dissolution into pentane, filtering through a Celite-lined frit, and removal of pentanes. TEMPO (2,2,6,6-tetramethylpiperidin-1-yl-oxyl) was sublimed under vacuum.[2] ^{t}Bu$_3$ArO$^•$ was prepared according to the literature method.[3] $[FeCp^*_2]PF_6$ was prepared by treatment of $FeCp^*_2$ with 1 equiv. of $[NO]PF_6$ in a benzene/acetonitrile mixture. $[(p\text{-tolyl})_3N]PF_6$ was prepared as described in the literature.[4] Sodium bis(trifluoromethane sulfonyl) imide (NaTFSI) was purified by the following procedures: (1) the NaTFSI suspension in dichloromethane was stirred for 6 h. After standing for 30 min, the upper solution was removed. (2) Procedure 1 was repeated 1 ten times. (3) NaTFSI was washed ten times with pentane, and then the solution was removed. (4) The solid was dried in a vacuum for 24 h. There was a small residual oxidizing impurity in the NaTFSI, 0.005 ± 0.001 mol%, that caused a small amount of oxidation of $CrCp^*_2$. To remove possible water molecules in Ti-based MOFs, MIL-125 and NH2-MIL-125 were dried at 200 °C in a vacuum oven.

MIL-125[8] and NH_2-MIL-125[9] were prepared by the reported procedures. MIL-125 of different sizes was prepared by using a controlled SBU approach described by patent EP 2398812B1. For the preparation of each material, the pivalate capped Ti_8O_8 inorganic cluster $Ti_8O_8(OOC^tBu)_{16}$ was used.[10]

NMR spectra were collected on Bruker 300, 500 or Agilent 400, 500 MHz spectrometers, and ^1H chemical shifts were referenced to residual solvent. Data were recorded with enough delay time and acquisition time for allowing full relaxation of methylene signals of [2.2.2]-cryptand and *p*-tolyl ether. Chemical shifts were reported relative to TMS by referencing the residual solvent. MestReNova© (version 9.0.0) was used to deconvolute the overlapping peaks using the Line Fitting tools. The peak heights, widths, areas and the ratios of Gaussian to Lorentzian line-shapes were allowed to vary based on minimizing the residual. All of average data and error (i.e. standard deviation) were calculated from three NMR experiments.

EPR spectra were collected on a Bruker EMX CW X-band spectrometer outfitted with a cryo-cooled cavity. Spectra of MOFs were collected from solid samples (7 – 19 mg) at 107 K at 9.29 GHz. Spectra of reduced molecular clusters were collected in a toluene glass (1-2 mM) at 111 K at 9.29 GHz. EPR spectra of the reduced clusters were fit to a Lorentzian using the W95EPR program (Monte Carlo fit).[7]

Optical spectroscopy measurements were taken on a Hewlett-Packard 8453 diode array spectrophotometer equipped with a Unisoku sample holder that has a temperature controller and magnetic stirrer. Unless noted, all optical spectroscopy measurements were done in MeCN. Samples were taken using quartz cuvettes sealed to a Teflon valve (Kontes) and 14/20 ground-glass joint.

B. X-ray Crystallography Measurements

Low-temperature diffraction data for $[Ti_8O_8(OOC^tBu)_{16}]Na(THF)_2$ were collected on a Bruker APEXII single crystal diffractometer coupled to a Bruker APEXII CCD detector with graphite-monochromated Mo Kα radiation (λ = 0.71073 Å), performing φ-and ω-scans at 100 K. The structures were solved by direct or Patterson methods using SHELXS[3] and refined against F^2 on all data by full-matrix least squares with SHELXL-97.[4] All non-hydrogen atoms were refined anisotropically. All hydrogen atoms were included into the model at geometrically calculated positions and refined using a riding model. The isotropic displacement parameters of all hydrogen atoms were fixed to 1.2 times the U value of the atoms they are linked to (1.5 times for methyl groups). The structure was refined using established methods.[5]

Low-temperature diffraction data for $[Ti_8O_8(OOC^tBu)_{16}]CoCp^*_2$ was collected at a crystal-to-detector distance was 60 mm and exposure time was 60 seconds per frame using a scan width of 1.0°. Data collection was 100.0% complete to 25.000° in θ. A total of 66708 reflections were collected covering the indices, -23<=*h*<=23, -19<=*k*<=13, -45<=*l*<=35. 6759 reflections were found to be symmetry independent, with an R_{int} of 0.0835. Indexing and unit cell refinement indicated a primitive, tetragonal lattice. The space group was found to be P 4/n c c (No. 130). The data were integrated using the Bruker SAINT software program and scaled using the SADABS software program. Solution by iterative methods (SIR-2011) produced a complete heavy-atom phasing model consistent with the proposed structure. All non-hydrogen atoms were refined anisotropically by full-matrix least-squares (SHELXL-2013). All hydrogen atoms were placed using a riding model. Their positions were constrained relative to their parent atom using the appropriate HFIX command in SHELXL-2013. SAME restraints were used to treat all disordered ^{t}Bu groups, keeping bond distances and angles similar using an esd of 0.02. SQUEEZE was used to treat the disordered $[CoCp^*_2]^+$, which sat on a crystallographically imposed 4-fold symmetry operation, as well as disordered MeCN solvent occupying the 6706 Å^3 of void space within the unit cell. The molecular formula, weight, density, and F(000) have been updated to reflect the estimated composition of the void space.

Data for these crystal structure(s) have been deposited and can be found as:

CCDC 1868235

CCDC 1868236

C. Synthesis of MOFs and Clusters

MIL-125 of different sizes was prepared by using a modified procedure to the controlled SBU approach described by patent EP 2398812B1. For the preparation of each material, the pivalate capped Ti_8O_8 inorganic cluster $Ti_8O_8(OOC^tBu)_{16}$ was used.[10]

MIL-125(Ti), batch 1. 3 g Terephthalic acid was dissolved in 50 mL of hot DMF (solution a) and simultaneously, 2.4 g of $Ti_8O_8(OOC^tBu)_{16}$ was dissolved in a mixture of 25 ml methanol and 50 mL DMF (solution b) and put in a sonication bath until full dissolution. After cooling down to room temperature, solution a was mixed with solution b in a Schott® pressure plus bottle of 250 ml and placed in a pre-heated oven of 100°C for 4 days. After the synthesis, the white powder was recovered by centrifugation and thoroughly washed with hot DMF (2 x 250 mL), to remove any unreacted terephthalic acid, and methanol (3 x 100 mL) to displace any adsorbed DMF. After the last washing steps, the powder was dried under vacuum at 60°C.

Small crystals of MIL-125(Ti), batch 2. Small, sphere like MIL-125(Ti) crystals with sizes between 150 and 250 nm were synthesized by adding 5 molar equivalents of excess benzoic acid as a modulator using the same synthesis protocol as for the normal MIL-125(Ti).

Large crystals of MIL-125(Ti), batch 3. Large, octahedral MIL-125(Ti) crystals with larger crystal sizes between 2 and 5 μm were synthesized by adding 3 molar equivalents of excess benzoic acid as a modulator using the same synthesis protocol as for the normal MIL-125(Ti).

MIL-125(Ti) deuterated, batch 4. MIL-125(Ti) with deuterated terephthalic rings was synthesized as the normal MIL-125(Ti) by replacing terephthalic acid by d_4-terephthalic acid.

NH_2-MIL-125(Ti). 11.9 g of 2-aminoterephthalic acid and 10.2 mL tetrabutyl titanate were dissolved in a mixture of 250 mL DMF, 50 mL methanol and 10 mL of acetic acid. The solution was subsequently refluxed for 24h and after the synthesis, the yellow powder was recovered by centrifugation and thoroughly washed with hot DMF (2 x 250 mL), to remove any unreacted linker, and methanol (3 x 100 mL) to displace any adsorbed DMF. After the last washing steps, the powder was dried under vacuum at 60°C.

Synthesis of $[Ti_8O_8(OOC^tBu)_{16}]Na(THF)_2$. A solution of $Ti_8O_8(OOC^tBu)_{16}$ (206.2 mg, 0.09686 mmol) in ~ 6 mL THF was added to a stirring 0.22 wt % Na/Hg amalgam (1.0676 g, 0.1017 mmol). An immediate color change from colorless to blue was noted. The solution was vigorously stirred for 6 h, after which the volatiles were removed by vacuum. The resulting blue solids were taken up in ~ 5 mL THF, filtered through a Celite-lined frit, and layered with MeCN (~ 10 mL). Crystals suitable for XRD were obtained (crop 1: 158.5 mg, 71.3 %). Concentration of the mother liquor and crystallization by addition of acetonitrile gives a second crop. ^1H NMR (d_8-THF, 500 MHz): **δ** 3.62 (m, overlapping with solvent, 8H), 1.76 (m, overlapping with solvent, 8H), 1.415 (s, 72 H), 1.234 (s, 72 H). (d_8-toluene, 700 MHz): **δ** 3.74 (bs), 1.63 (bs), 1.530 (s, 72 H), 1.416 (s, 72 H). (C_6D_6, 300 MHz): **δ** 3.63 (bs), 1.63 (bs), 1.559 (s, 72 H), 1.458 (s, 72 H). UV-vis (C_6H_6) λ_{max}, nm (ε, M^{-1} cm^{-1}): 414 (sh, 220), 515 (450), 790 (680). EPR (toluene, 111 K): g = [1.950, 1.904, 1.781]; W = [53.0, 56.0, 81.0]. Anal. Calcd. for $Ti_8O_{42}C_{88}H_{160}Na$: C 46.0; H 7.02; N 0. Found: C 45.96; H 7.12; N < 0.02.

Synthesis of $[Ti_8O_8(OOC^tBu)_{16}]CoCp^*_2$. To a stirring solution of $Ti_8O_8(OOC^tBu)_{16}$ (126.2 mg, 0.0593 mmol) in ~ 3 mL benzene was added a solution of $CoCp^*_2$ (20.5 mg, 0.0622 mmol) in ~ 3 mL benzene. The solution immediately became blue. The solution was stirred for 20 min, after which the volatiles were removed be vacuum. The resulting blue solids were taken up in ~ 1 mL THF, filtered through a Celite-lined pipette, and layered with MeCN (~ 2 mL). Crystals suitable for XRD were obtained (55.8 mg, 38.3 %). ^{1}H NMR (d_8-THF, 500 MHz): **δ** 1.79 (s, 30H), 1.373 (s, 72 H), 1.217 (s, 72 H). (d_8-toluene, 500 MHz): **δ** 1.617 (s, 72H), 1.457 (bs, overlapping with singlet at 1.433), 1.433 (s, overlapping with singlet at 1.457). (C_6D_6, 500 MHz): **δ** 1.656 (s, 72H), 1.500 (s, 72 H), 1.401 (s, 30H). UV-vis (C_6H_6) λ_{max}, nm (ε, M^{-1} cm^{-1}): 410 (sh, 580), 5 15 (470), 790 (630). EPR (toluene, 111 K): g = [1.919, 1.899, 1.783]; W = [98.0, 228, 258]. Anal. Calcd. for $Ti_8O_{40}C_{100}H_{174}Co$: C 48.85; H 7.13; N 0. Found: C 48.72; H 7.17; N < 0.02.

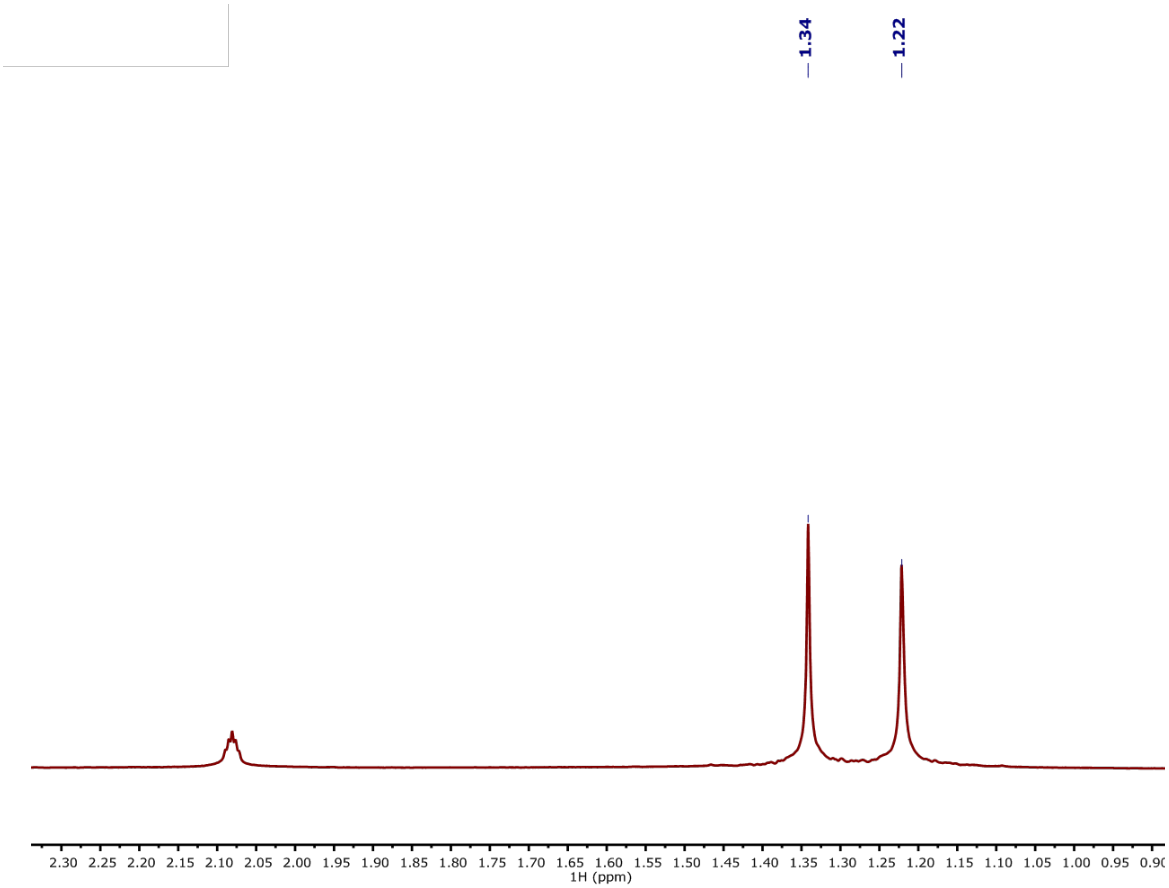

Figure S1. ^{1}H NMR spectrum (500 MHz, d_8-toluene,) of $Ti_8O_8(OOC^tBu)_{16}$ (1). The peaks at 1.34 and 1.22 ppm correspond to the cluster ^{t}Bu protons; the assignment of the equatorial and axial resonances is not known. Peak at 2.08 is due to toluene.

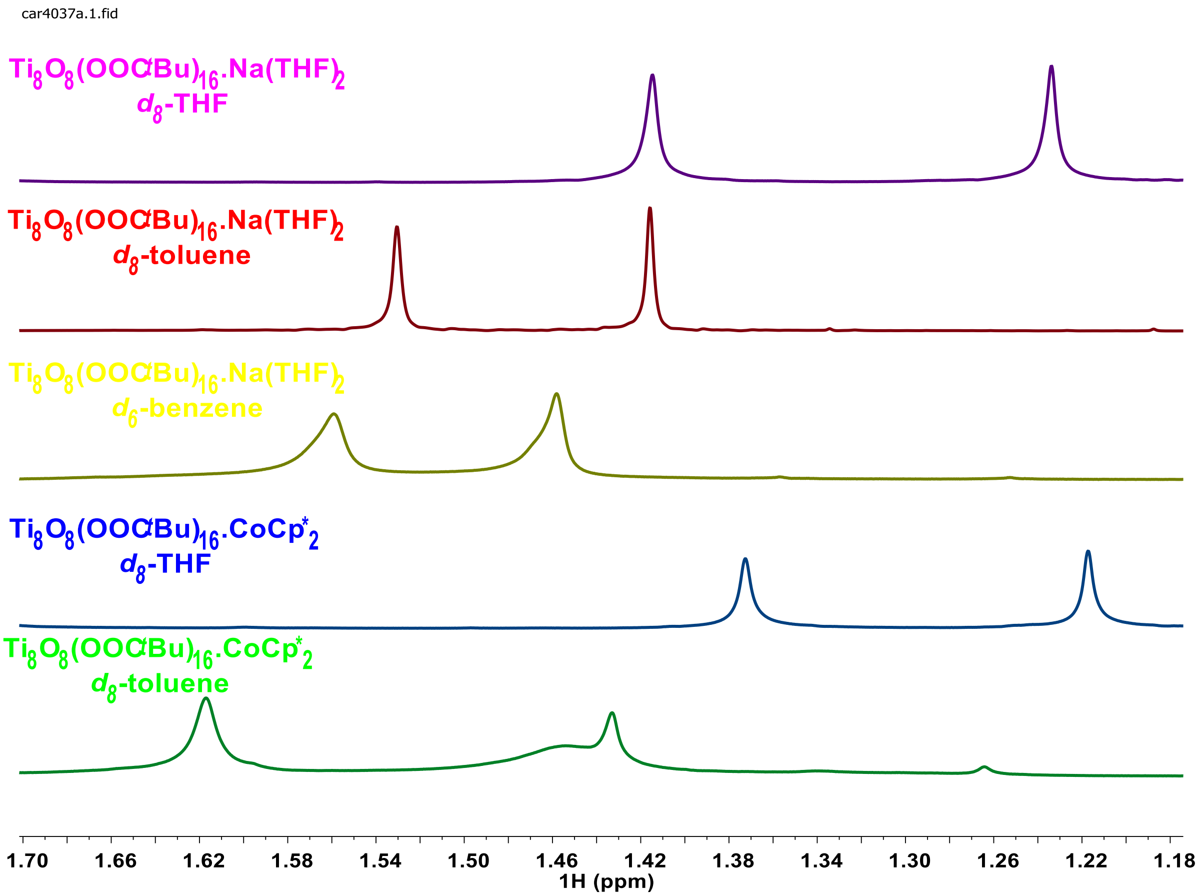

Figure S2. Stacked ^{1}H NMR spectra of $Ti_8O_8(OOC^tBu)_{16}^-$ showing the effect of solvent and counter-cation.

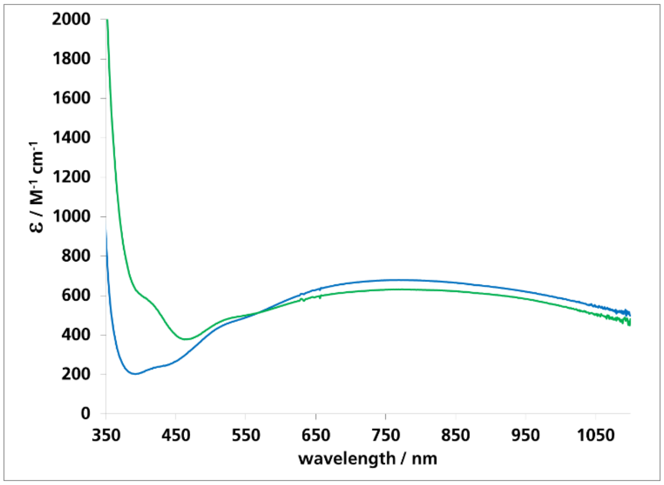

Figure S3. UV-vis spectra of $[Ti_8O_8(OOC^tBu)_{16}]Na(THF)_2$ (blue) and $[Ti_8O_8(OOC^tBu)_{16}]CoCp^*_2$ (green) in benzene.

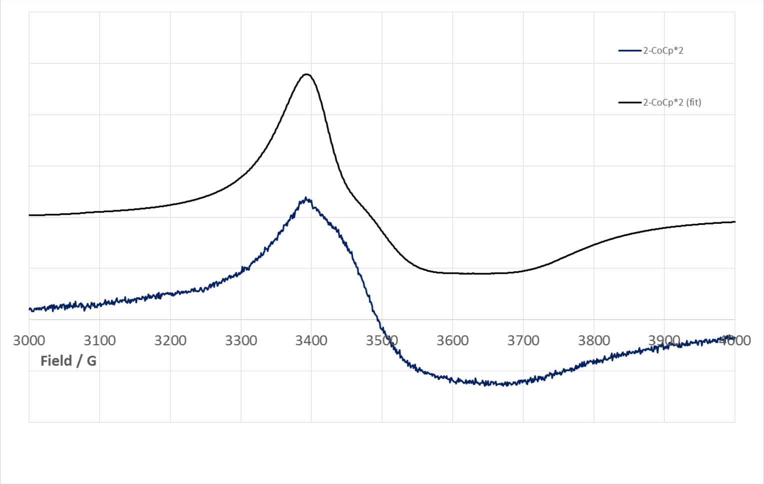

Figure S4. EPR spectrum of **2-CoCp$^*_2$** collected at 111K as a toluene glass (blue trace). The spectrum was fit (black trace) using the following parameters: g = [1.919, 1.899, 1.783]; W = [98.0, 228, 258].

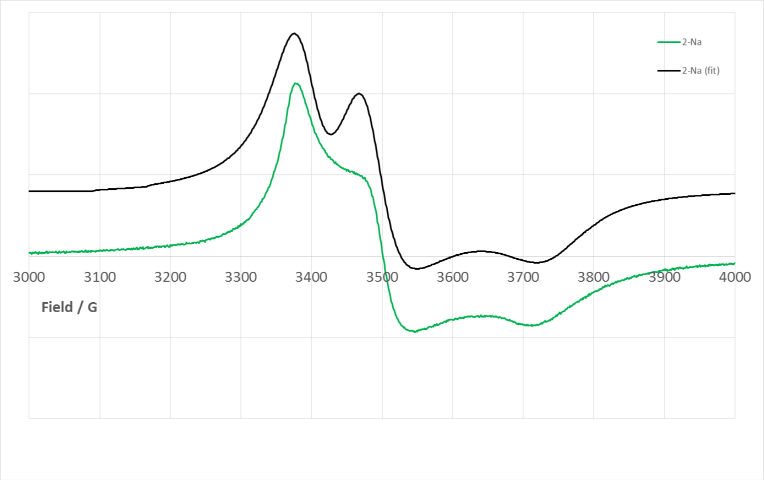

Figure S5. EPR spectrum of **2-Na** collected at 111K as a toluene glass (green trace). The spectrum was fit (black trace) using the following parameters: g = [1.950, 1.904, 1.781]; W = [53.0, 56.0, 81.0].

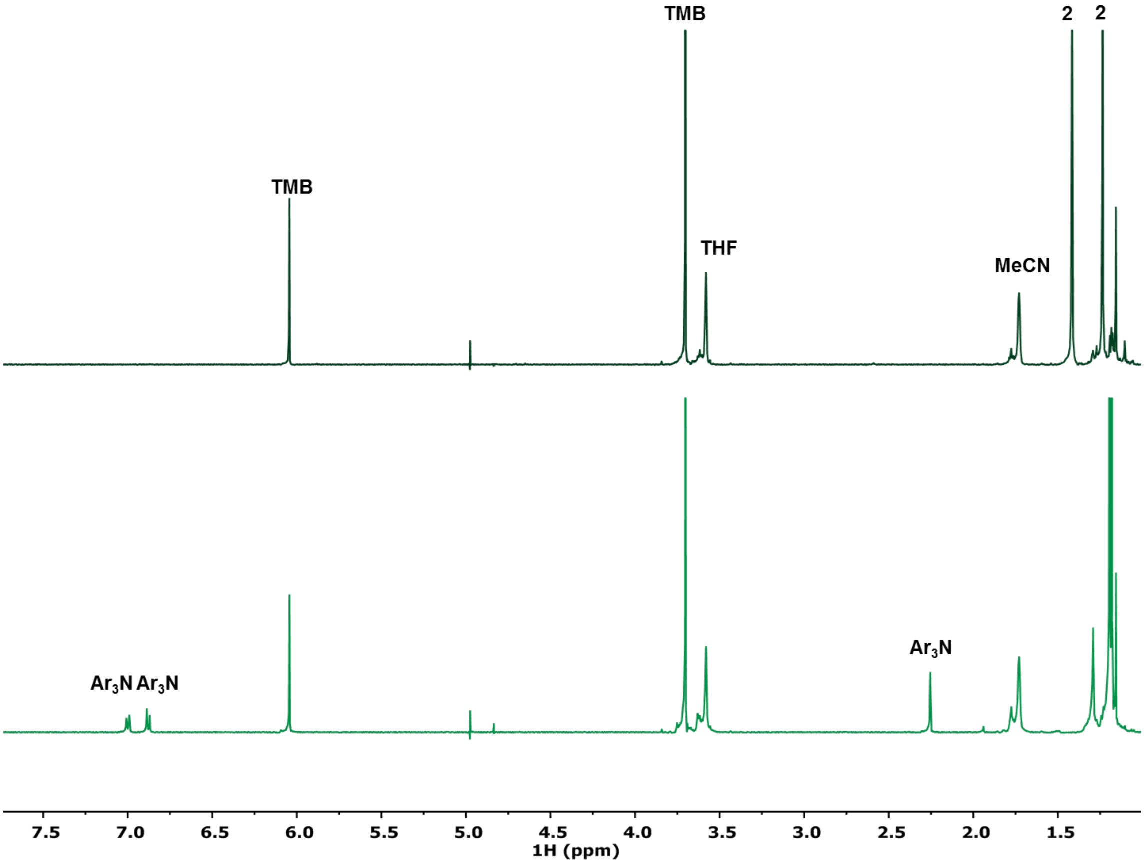

Figure S6. Stacked ^{1}H NMR spectra (d_8-THF, 300 MHz) of (top): **2-Na**; (bottom): **2-Na** + 1 equiv. *p*-tolyl$_3$N$^{\bullet +}$. TMB (1,3,5-trimethoxybenzene) was used as an internal standard.

D. Powder XRD

Powder X-ray diffraction patterns were recorded on a STOE COMBI P diffractometer (monochromated CuKα-radiation, λ = 1.54060 Å) equipped with an IP-PSD detector in transmission geometry.

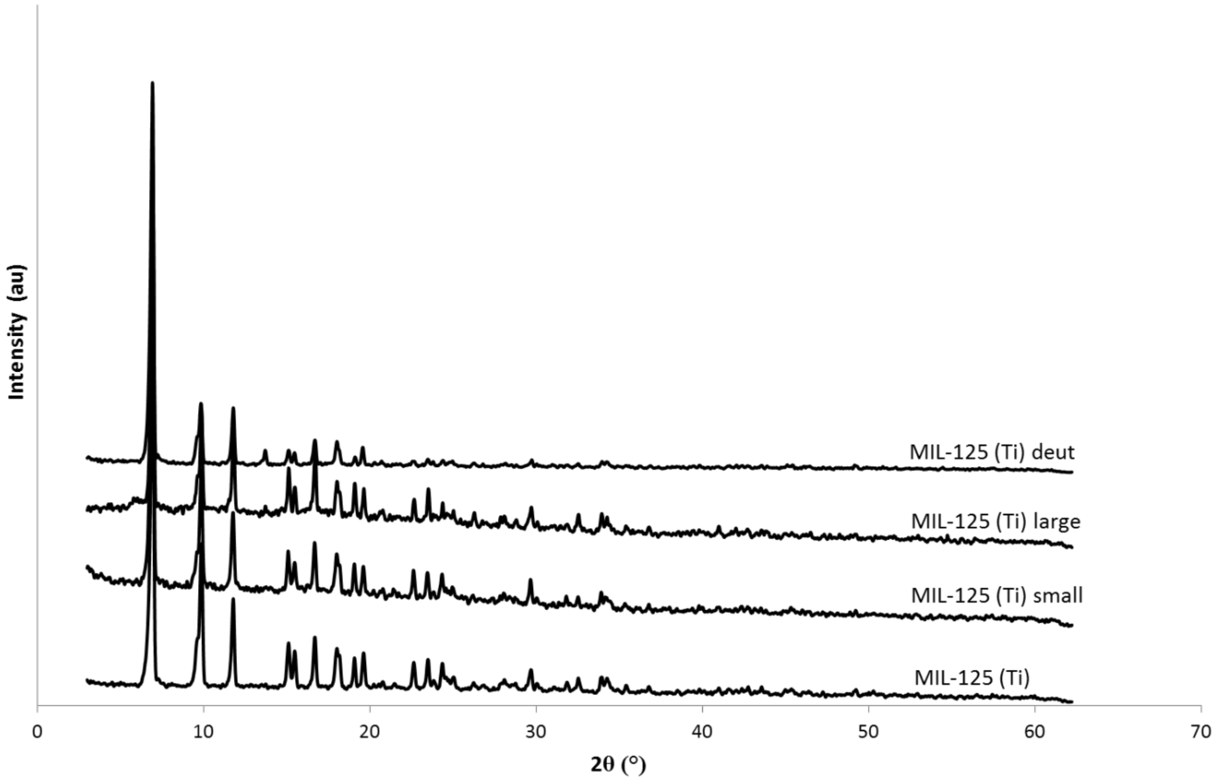

Figure S7. Powder X-ray diffractograms of the different MIL-125(Ti) syntheses.

Following reduction of MIL-125 by varying amounts of $CoCp_2^*$, diffraction patterns were recorded to assess the structural integrity of the materials. Structureless Pawley fits were performed on these patterns using TOPAS v6. Patterns were fitted between 2 ° and 50 ° 2θ. Backgrounds were fitted with a 10th-order Chubychev polynomial, and a Thompson-Cox-Hastings pseudo-Voigt function was employed as profile function. From the fits in Figures S9-S11, it is clear that even up to a complete reduction of the material (i.e., 8 e^- per Ti_8 cluster) MIL-125's structure is retained. However, the appearance of an additional set of reflections, most notably at 10.4 °, 13.9° and 17.7 ° 2θ, which are not allowed for MIL-125 (space group *I4/mmm*) indicate the formation of a second phase upon reduction, likely indicating some structural instability of MIL-125 towards the reduction reaction with $CoCp_2^*$. Indexing of these reflections did not yield a plausible unit cell or structure to identify this additional phase.

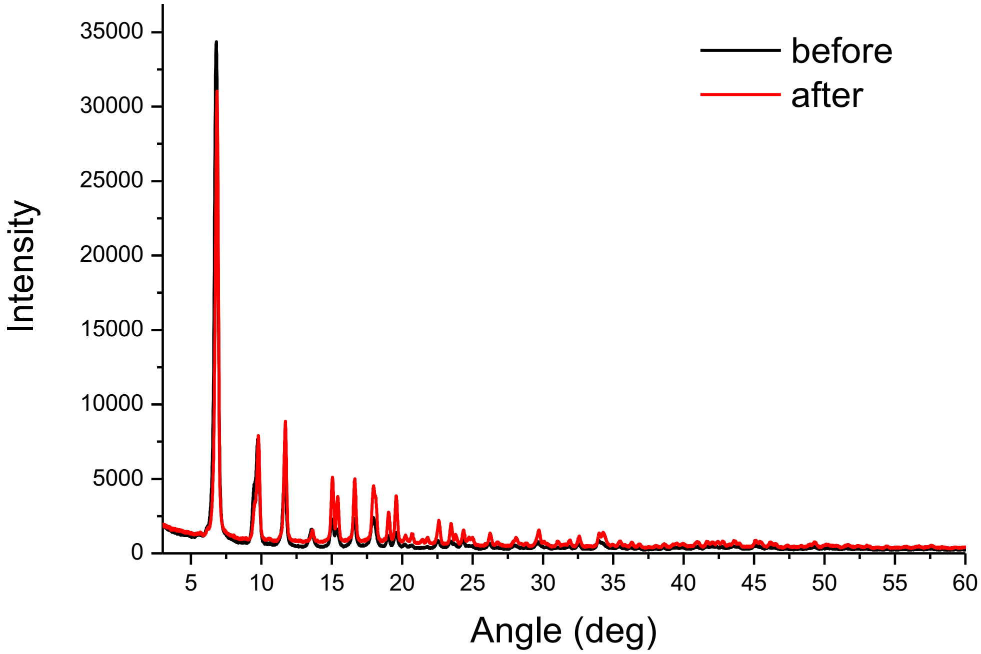

Figure S8. Powder XRD diffractograms of MIL-125 upon 2.2 e- reduction ("before, black") and after re-oxidation.

1 e^--reduced MIL-125

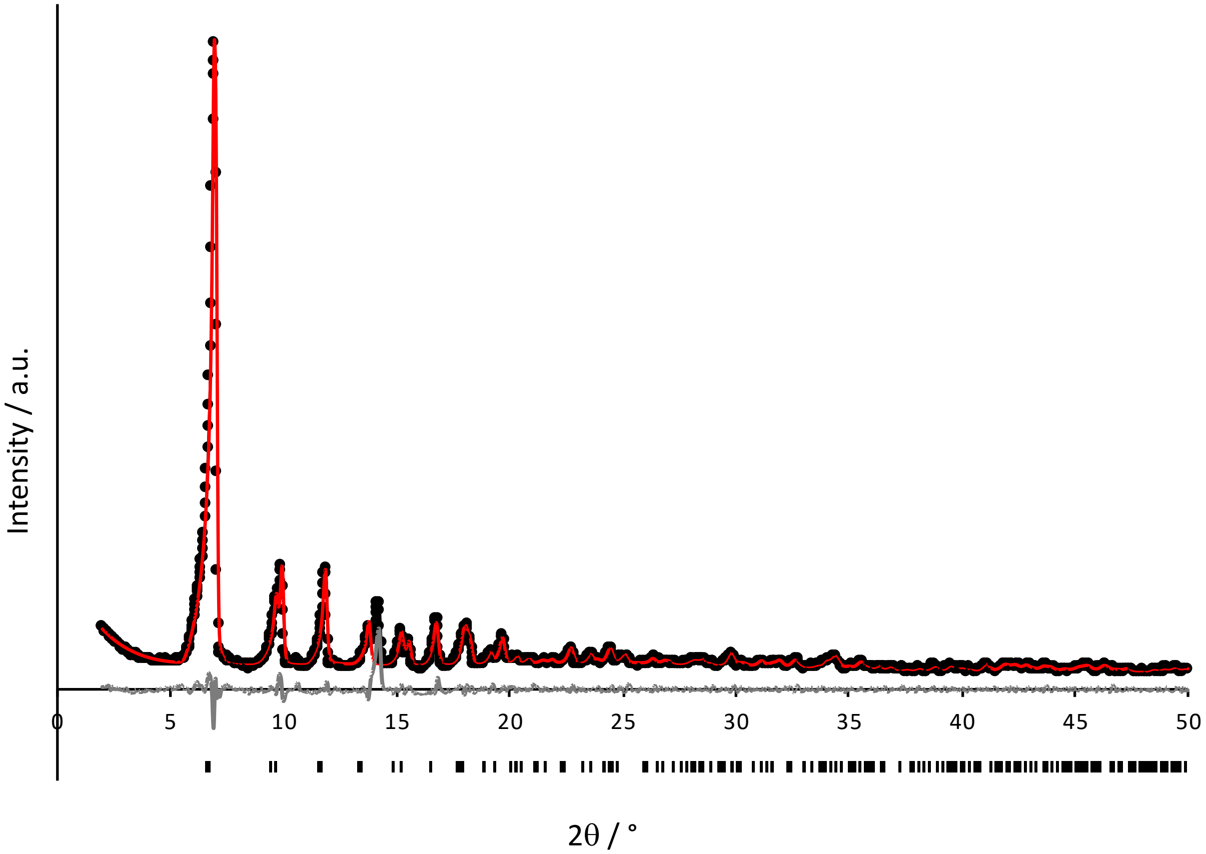

Figure S9: Pawley fit of 1 e^--reduced MIL-125. Measured data is represented by black dots, whereas the red and gray traces represent the calculated and difference data, respectively. Space group *I*4*/mmm* (n° 139); $a = b = 18.6771(79)$ Å; $c = 18.2007(84)$ Å; $\alpha = \beta = \gamma = 90$ °; V = 6349 Å^3; $R_{wp} = 9.197$; $R_{exp} = 1.377$.

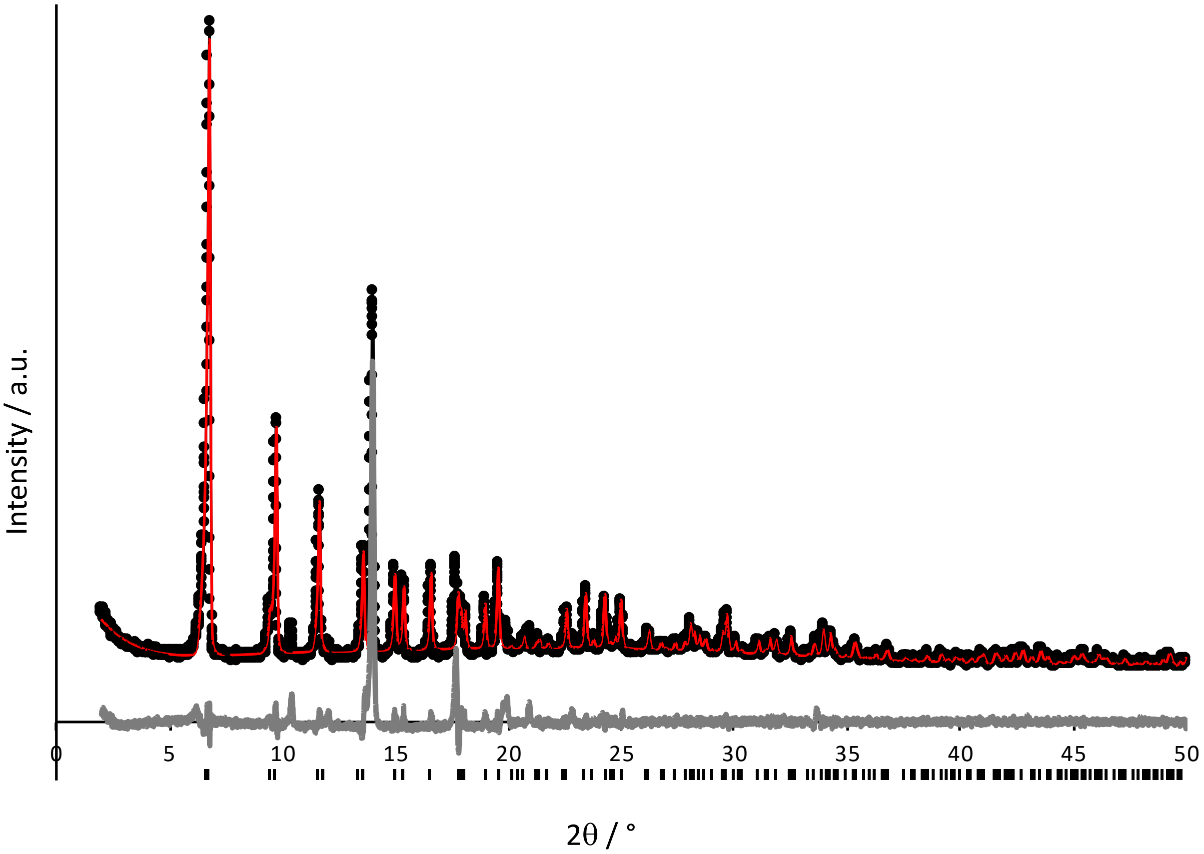

Figure S10: Pawley fit of 2 e^--reduced MIL-125. Measured data is represented by black dots, whereas the red and gray traces represent the calculated and difference data, respectively. Space group *I*4/*mmm* (n° 139); $a = b = 18.6712(30)$ Å; $c = 18.1248(31)$ Å; $\alpha = \beta = \gamma = 90$ °; V = 6318 Å^3; $R_{wp} = 11.962$; $R_{exp} = 1.808$.

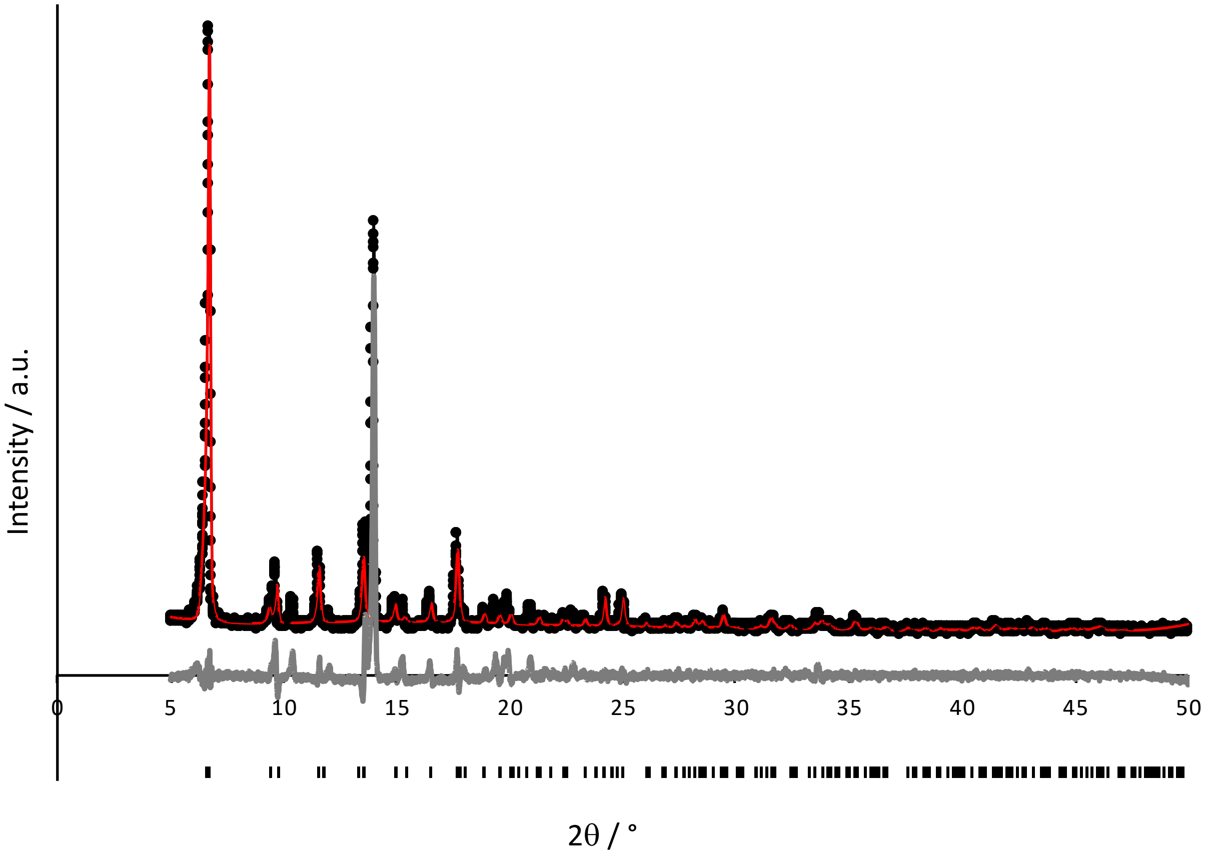

Figure S11: Pawley fit of 8 e^--reduced MIL-125. Measured data is represented by black dots, whereas the red and gray traces represents the calculated and difference data, respectively. Space group *I*4/*mmm* (n° 139); $a = b = 18.6999(72)$ Å; $c = 18.0691(78)$ Å; $\alpha = \beta = \gamma = 90$ °; V = 6318 Å^3; $R_{wp} = 15.102$; $R_{exp} = 2.866$.

E. SEM Images

Scanning electron microscopy (SEM) images were recorded on a Philips XL30 FEG microscope, the samples were coated with Au before imaging.

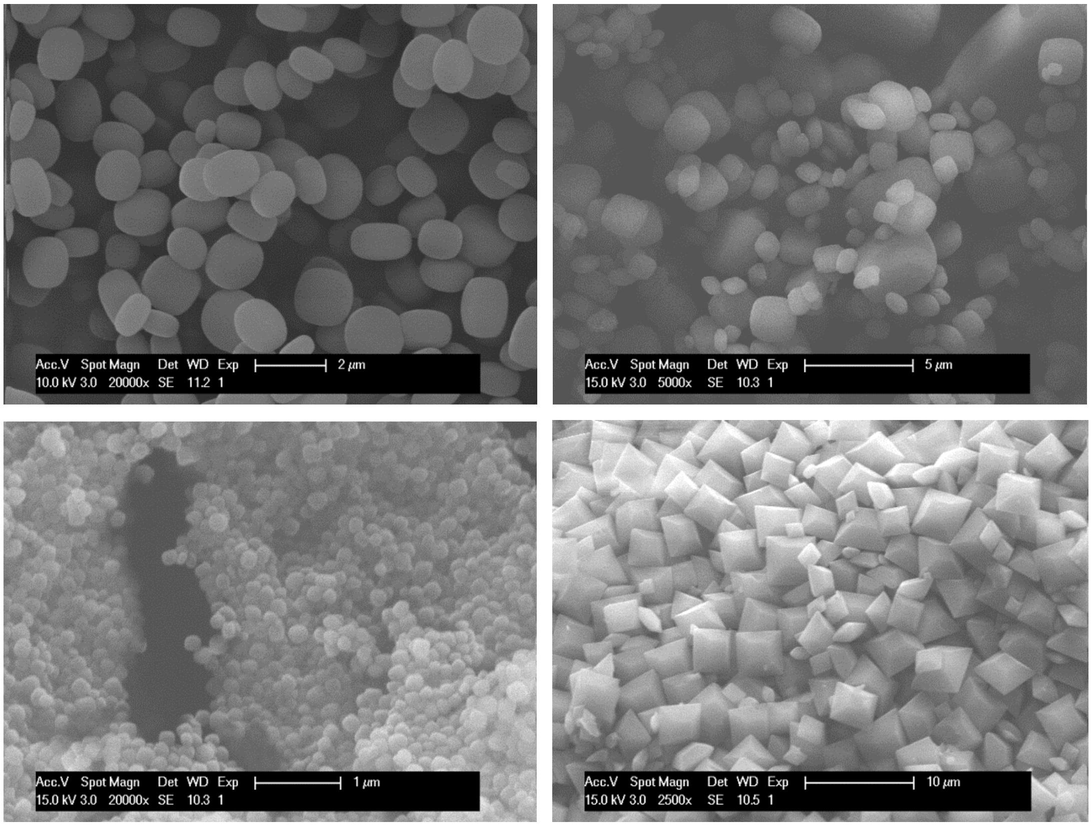

Figure S12: SEM pictures of (top left) MIL-125, batch 1 (top right) MIL-125 deuterated, batch 4 (bottom left) small crystals of MIL-125, batch 2 and (bottom right) large crystals of MIL-125, batch 3.

F. Size Analysis

Size and morphology of MIL-125 crystals were taken from the SEM images (Figure S12). Batches 1 and 4 have ellipsoid morphologies, whilst batch 2 has spherical morphology and that of batch 3 was taken to be octahedron. From the images, the average radii (with error taken to be from the size distribution in the images) were measured and used to obtain the volume of the crystallites. The outer shell was assumed to have a thickness equal to the shortest intercluster Ti-Ti distance + the longest Ti-Ti intracluster distance (1.088 and 0.8247 nm, respectively).[8] From this, the volume of the entire cluster and that of the interior could be calculated, to give the fraction of Ti_8 clusters within the outer shell (Table S1). This can be used to determine the extent of reduction of the outer shell Ti_8 clusters, if reduction occurred exclusively at the surface with no migration of charge to the interior.

Table S1. Calculation of size/volume and fraction of Ti_8 clusters in outer shell of MIL-125 crystallites. The large error in volume for batches 3 and 4 are due to the large size distribution.

			axes / nm			error / nm					Fraction in outer shell		Assuming all reduction occures in outer shell only:
Batch	**Morphology**	**a**	**b**	**c**	**a (error)**	**b (error)**	**c (error)**	**Volume / nm^3**	**Volume (error) / nm^3**	**$Volume_{interior}$**	**(Volume-$Volume_{interior}$)/Volume**	**# e^- in outer shell (1 e^- reduced)**	**# e^- in outer shell (2 e^- reduced)**
1	ellipsoid	850.00	700.00	300.00	50.00	100.00	100.00	7.48E+08	4.60E+08	7.39E+08	0.0113	88.34	176.67
2	sphere	85.00	85.00	85.00	16.50	16.50	16.50	2.57E+06	1.80E+06	2.40E+06	0.0660	15.15	30.30
3	octahedron	2650.00			1350.00			8.77E+09	2.14E+10	8.73E+09	0.0045	221.17	442.33
4	ellipsoid	1150.00	1150.00	600.00	350.00	350.00	200.00	3.32E+09	4.22E+09	3.30E+09	0.0065	153.82	307.65

G. MOF Uptake Studies

Studies concerning uptake of materials into MIL-125 were included in a companion paper;[11] the text in this section is repeated here for completeness.

In the glovebox, stock solutions of ^{t}Bu$_3$ArOD (20 mM), TEMPOH (40 mM), FeCp$^*_2$ (20 mM), FeCp$_2$ (40 mM), (*p*-tolyl)$_2$O (40 or 80 mM), diphenylmethanol (40 mM), (*p*-tolyl)$_3$N (40 mM), and (*p*-tolyl)$_2$CHOH (80 mM) were prepared in C_6D_6. The following were added to 5 NMR tubes:

A. 100 μL TEMPOH, 100 μL (*p*-tolyl)$_2$O (40 mM), 200 μL FeCp$^*_2$, 100 μL C_6D_6
Final concentration: 8 mM each

B. 200 μL FeCp$_2$, 200 μL ^{t}Bu$_3$ArOD, 100 μL diphenylmethanol
Final concentration: 16 mM FeCp$_2$ and 8 mM for the others

C. 100 μL diphenylmethanol, 100 μL TEMPOH, 200 μL ^{t}Bu$_3$ArOD
Final concentration: 8 mM each

D. 100 μL FeCp$_2$, 200 μL FeCp$^*_2$, 200 μL (*p*-tolyl)$_2$O (40 mM)
Final concentration: 16 mM FeCp$_2$ and 8 mM for the others

E. 400 μL (*p*-tolyl)$_3$N, 200 μL (*p*-tolyl)$_2$O (80 mM), 200 μL (*p*-tolyl)$_2$CHOH (80 mM)
Final concentration: 20 mM each

^{1}H NMR spectra for each sample were collected, and the tubes brought back into the glovebox. 4-6 mg of MIL-125 (batch 1) was added to tubes A-D, and 2.7 mg of MIL-125 (batch 1) was added to tube E. A stirring bar was added to the tubes, and the suspension stirred. After 3 h, the stirring bar was removed from samples A-D and the ^{1}H NMR spectra were collected. The samples were brought back into the box, and stirred for an additional 18.5 h, at which time the stir bar was removed and the ^{1}H NMR spectra collected again. Sample E was allowed to stir for 16.5 h at which point the stir bar was removed and the ^{1}H NMR spectrum collected.

Relative integration of the peaks that correspond to each species allowed for qualitative assessment of which substrates were taken up in the pores of MIL-125. These studies reveal that TEMPOH and diphenylmethanol fit in the pores (TEMPOH more so), and also (*p*-tolyl)$_2$CHOH. Neither FeCp$_2$ nor FeCp$^*_2$ fit in the pores, since their relative integrals were unchanged.

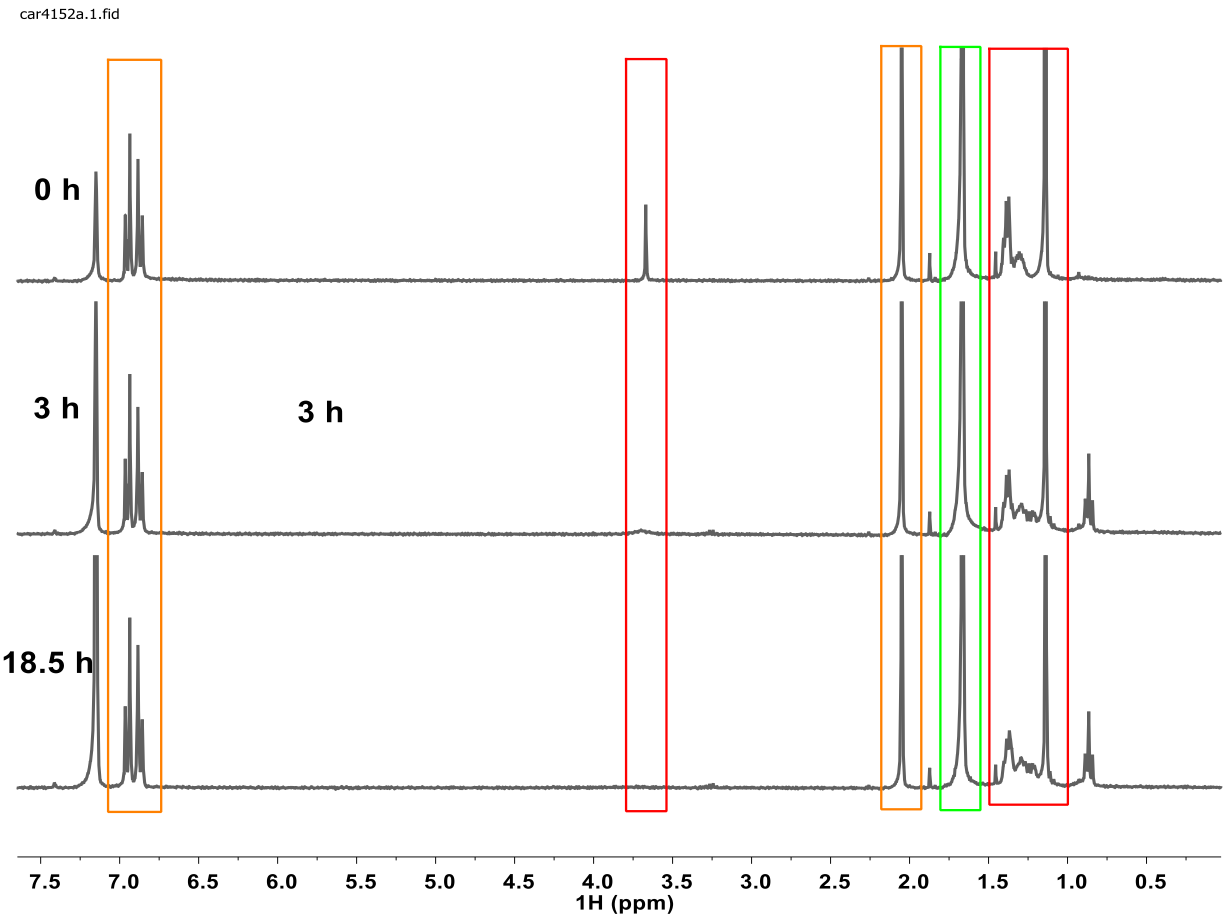

Figure S13. Stacked ^{1}H NMR Spectra (C_6D_6, 300 MHz) of sample A. Resonances ascribed to TEMPOH are in red, those of (*p*-tolyl)$_2$O in orange, and that of FeCp$^*_2$ in green.

Table S2. Relative integration of resonances for uptake study A. Fraction remaining from t = 0 value noted in parenthesis.

Time	TEMPOH (δ 3.67)	(*p*-tolyl)$_2$O (δ 2.05)	FeCp*$_2$ (δ 1.67)
0	0.86	6.00	30.45
3 h	0.43 (0.5)	6.00 (0)	31.05 (1.02)
21.5 h	0.13 (0.15)	6.00 (0)	29.99 (0.98)

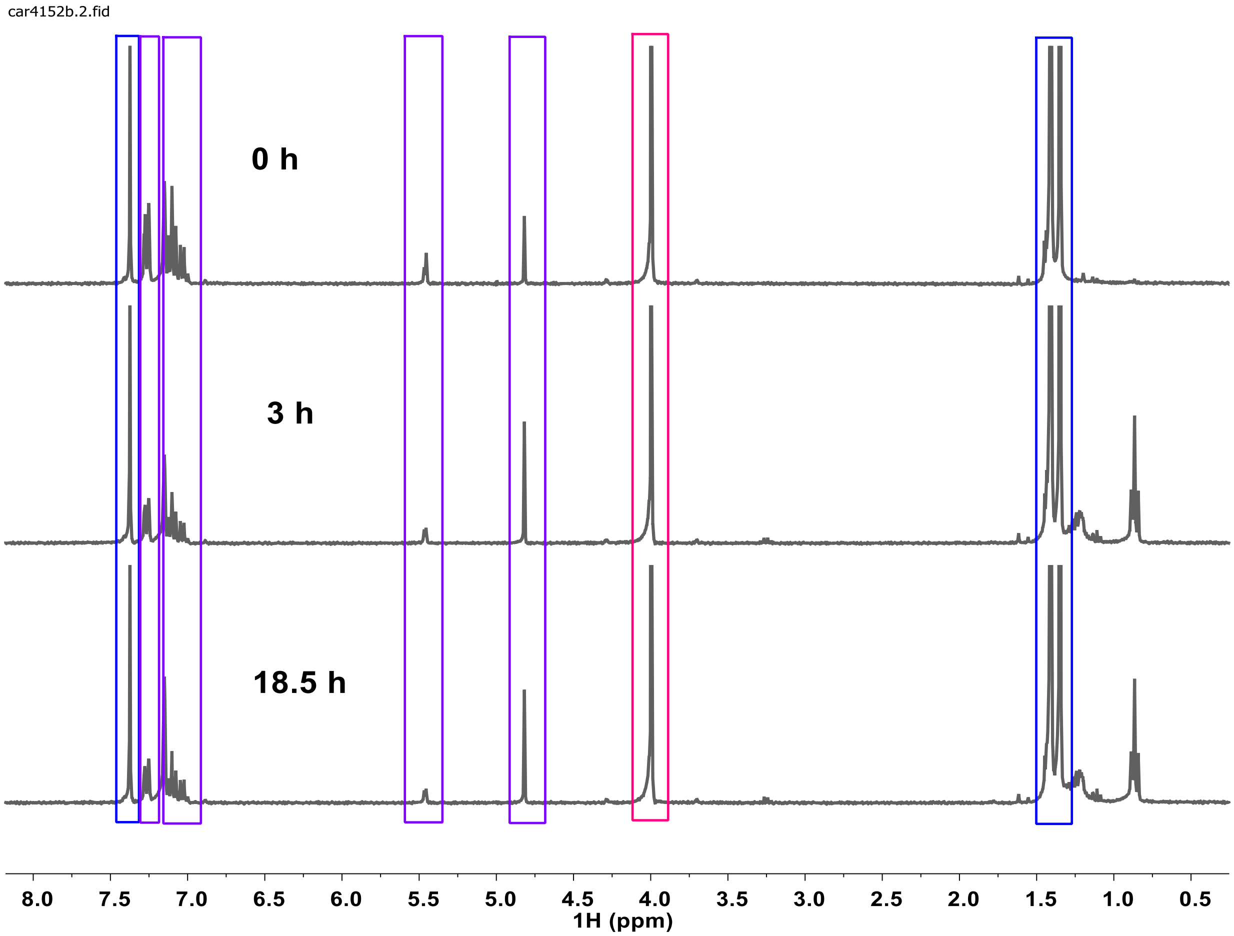

Figure S14. Stacked ^{1}H NMR Spectra (C_6D_6, 300 MHz) of sample B. Resonances ascribed to ^{t}Bu$_3$ArOD are in blue, those of diphenylmethanol in purple, and that of $FeCp_2$ in pink.

Table S3. Relative integration of resonances for uptake study B. Fraction remaining from *t* = 0 value noted in parenthesis.

Time	**^{t}Bu$_3$ArOD (δ 7.37)**	**diphenylmethanol (δ 7.26)**	**$FeCp_2$ (δ 4.00)**
0	2.00	2.31	5.55
3 h	2.00 (0)	1.20 (0.52)	5.67 (1.02)
21.5 h	2.00 (0)	1.33 (0.58)	5.93 (1.07)

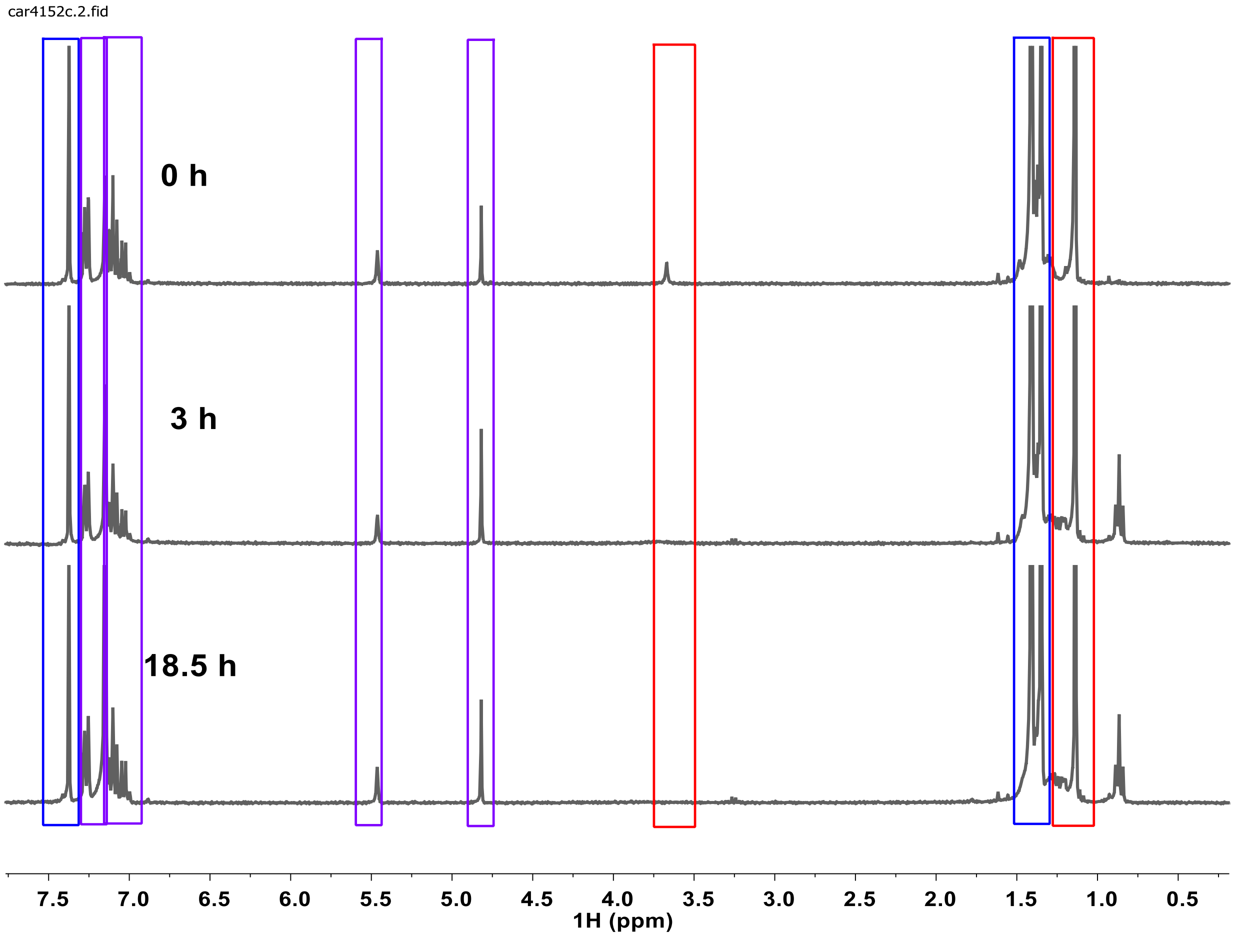

Figure S15. Stacked ^{1}H NMR Spectra (C_6D_6, 300 MHz) of sample C. Resonances ascribed to ^{t}Bu$_3$ArOD are in blue, those of diphenylmethanol in purple, and those of TEMPOH in red.

Table S4. Relative integration of resonances for uptake study C. Fraction remaining from $t = 0$ value noted in parenthesis.

Time	^{t}Bu$_3$ArOD (δ **7.37)**	diphenylmethanol (δ **7.26)**	**TEMPOH (δ 3.67)**
0	2.00	2.59	0.49
3 h	2.00 (0)	2.07 (0.80)	0.11 (0.22)
21.5 h	2.00 (0)	2.64 (1.02)	0.05 (0.10)

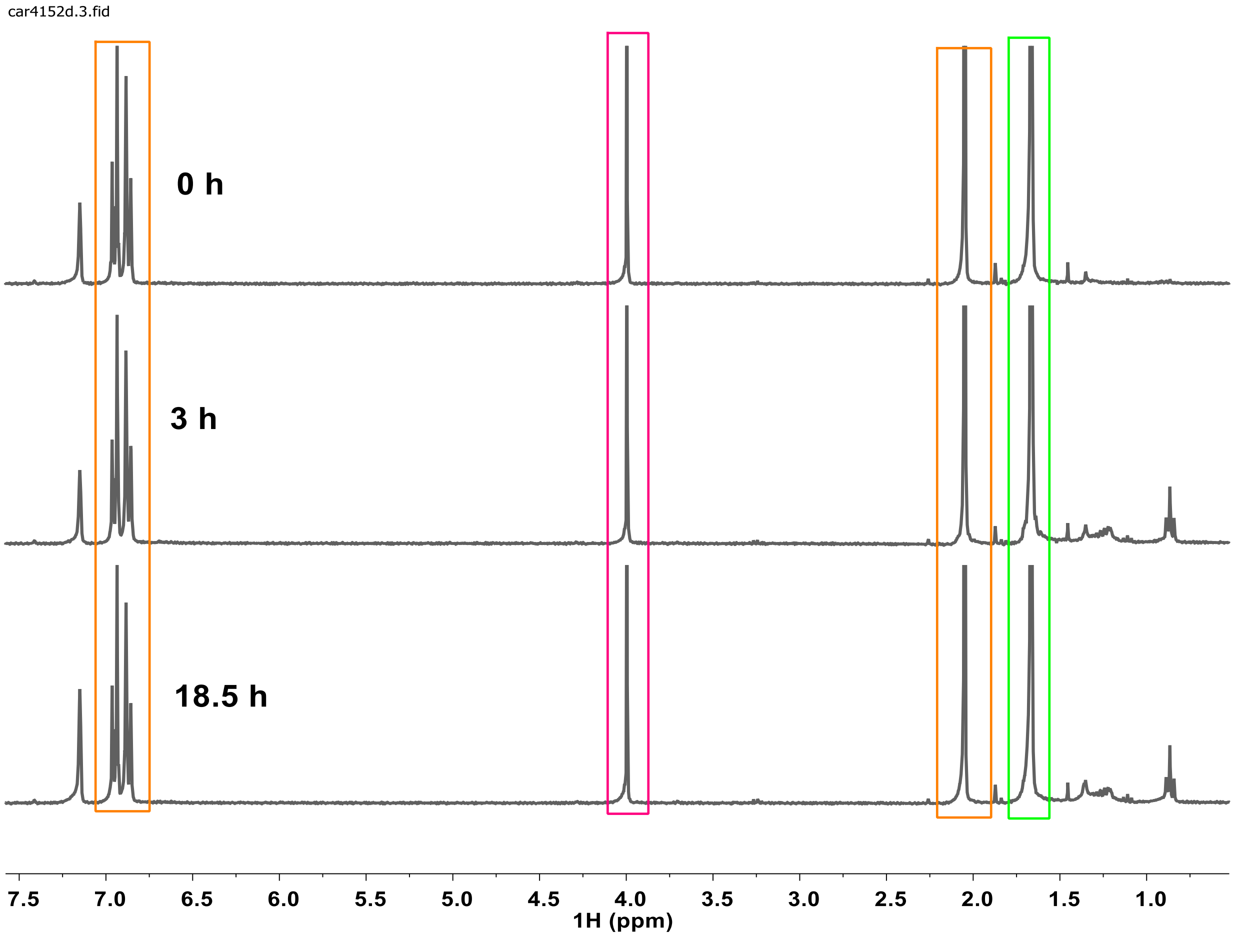

Figure S16. Stacked ^{1}H NMR Spectra (C_6D_6, 300 MHz) of sample D. Resonances ascribed to (*p*-tolyl)$_2$O are in orange, those of ^{t}Bu$_3$ArOD are in blue, that of FeCp$^*_2$ in green, and that of FeCp$_2$ in pink.

Table S5. Relative integration of resonances for uptake study D. Fraction remaining from *t* = 0 value noted in parenthesis.

Time	(*p*-tolyl)$_2$O (δ 2.05)	FeCp$_2$ (δ 4.00)	FeCp*$_2$ (δ 1.67)
0	6.00	1.53	14.30
3 h	6.00 (0)	1.52 (0.99)	15.40 (1.08)
21.5 h	6.00 (0)	1.81 (1.18)	15.30 (1.07)

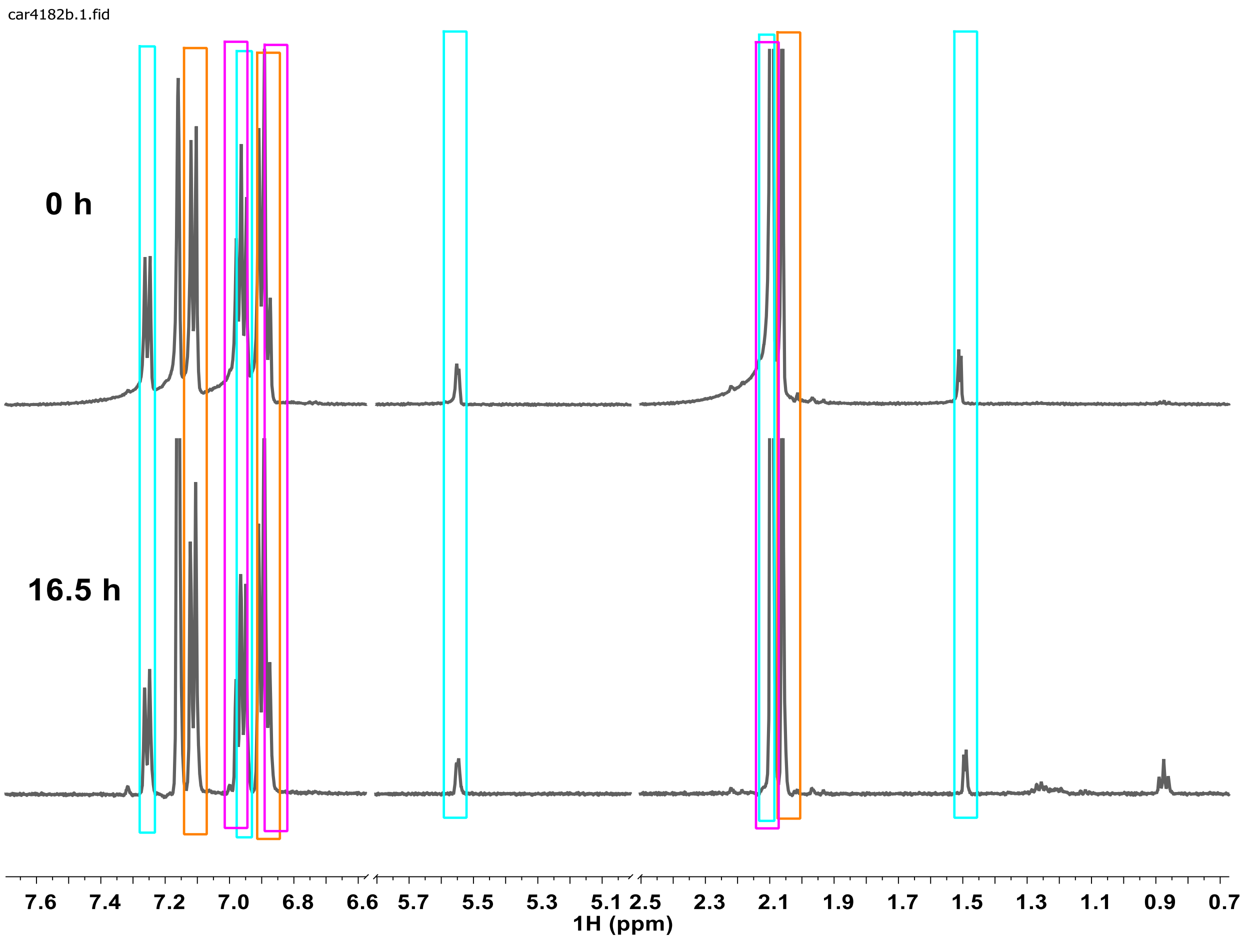

Figure S17. Stacked ^{1}H NMR Spectra (C_6D_6, 300 MHz) of sample E. Resonances ascribed to (*p*-tolyl)$_2$O are in orange, those of (*p*-tolyl)$_3$N are in magenta, and those of (*p*-tolyl)$_2$CHOH in cyan.

Table S6. Relative integration of resonances for uptake study E. Percent remaining from t = 0 value noted in parenthesis. All resonances of (*p*-tolyl)$_3$N overlapped with others, precluding analysis.

Time	(*p*-tolyl)$_2$O (δ 7.11)	(*p*-tolyl)$_2$CHOH (δ 7.25)
0	2	1.067
16.5 h	2 (0)	0.772 (0.72)

H. Chemical Reduction of MIL-125

H.1. Reduction with $CoCp^*_2$

In a typical experiment, in the glovebox, a known mass of MIL-125 (5.0 – 15.0 mg) was transferred to a scintillation vial containing a stirring bar. To this was added a THF solution of $CoCp^*_2$ (2 – 10 equiv, ~ 32 mM) and the reaction stirred. $NaBArF_{24}$ or $NaPF_6$ (0.5 – 10 equiv, ~ 12 mM) was then added as a THF solution. An immediate color change of the solids to dark purple was noticed upon addition of the sodium salt, concomitant with a lightening of the orange/brown solution. The reaction stirred for 15 h, after which the reaction was filtered through a pipette containing a glass filter paper. The solids were rinsed with THF, and the volatiles of the filtrate removed under vacuum. The remaining solids, as well as the filter, were transferred to another vial, and the solids were dried under vacuum (note, this often involved breaking the glass pipette, and hence transferring the glass with the solids). The solids from the filtrate were then taken up in d_3-MeCN, and the ^1H NMR spectrum collected. The insoluble dark solids were suspended in C_6D_6, and a known volume of a C_6D_6 solution containing $^tBu_3ArO^•$ (slight excess relative to the reducing equiv. added) and the Ar_2O internal standard. This solution was stirred for at least 5h. At this time, the solution was transferred to an NMR tube, and ^1H NMR analysis was done as described above. For reactions that had ≤ 2 equiv. $Na^+/CoCp^*_2$, a color change from dark purple to white occurred upon oxidation. For reactions that had > 2 equiv. $Na^+/CoCp^*_2$, the solids remained dark. Upon exposure to air, all chemically reduced samples changed color to white.

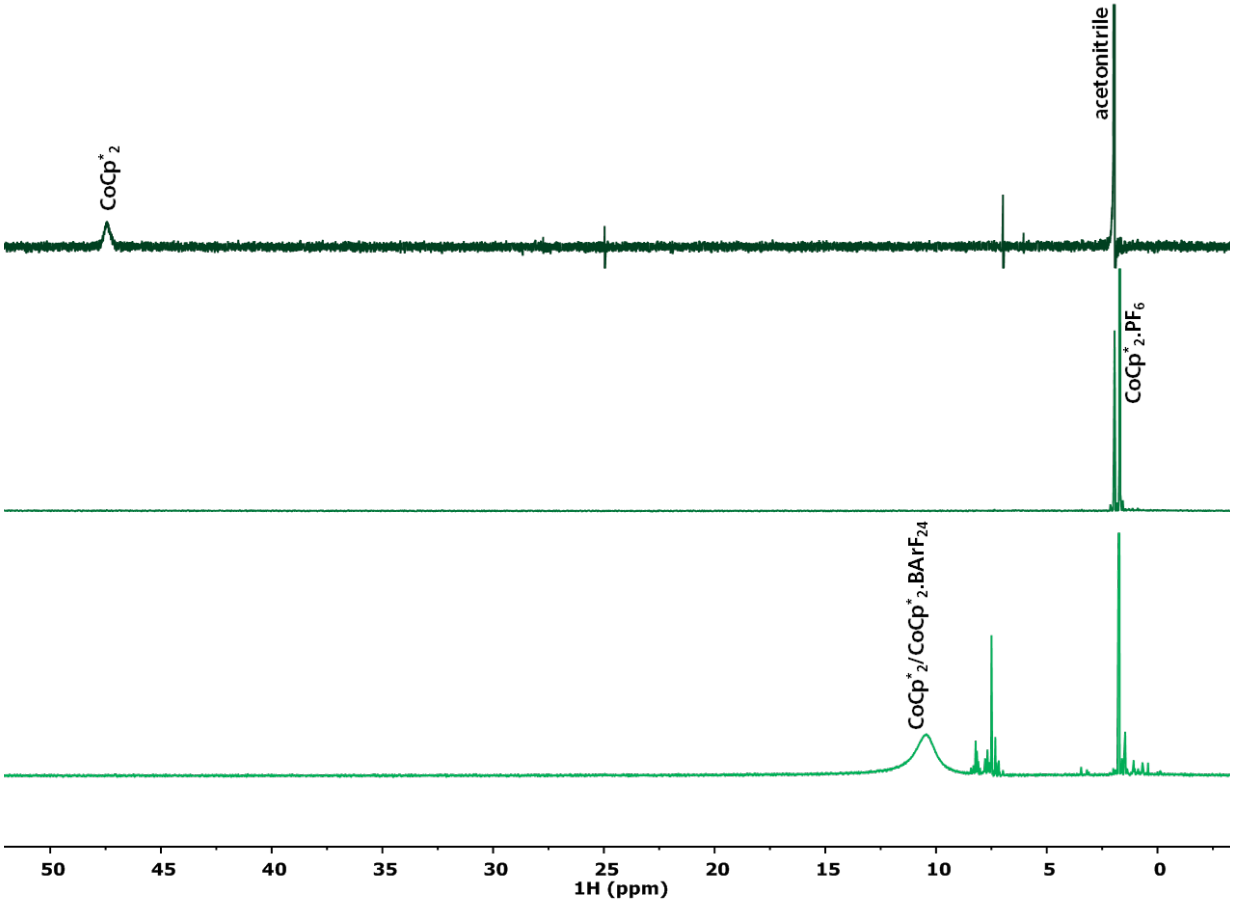

Figure S18. Exemplary ^{1}H NMR (500 MHz, d_3-MeCN) spectra of (top): CoCp$^*_2$ (47.4 ppm); (middle): [CoCp$^*_2$]PF$_6$ (1.70 ppm); mother liquor of the reaction of MIL-125 (batch 2) with 2 equiv. of CoCp$^*_2$ and 1.0 equiv. of NaBArF$_{24}$. Unlabeled peaks in the diamagnetic region correspond to solvent, BArF$_{24}^-$, and impurities from the NaBArF$_{24}$. From the chemical shift, MIL-125 was reduced by 1.6 e^-/Ti$_8$ cluster.

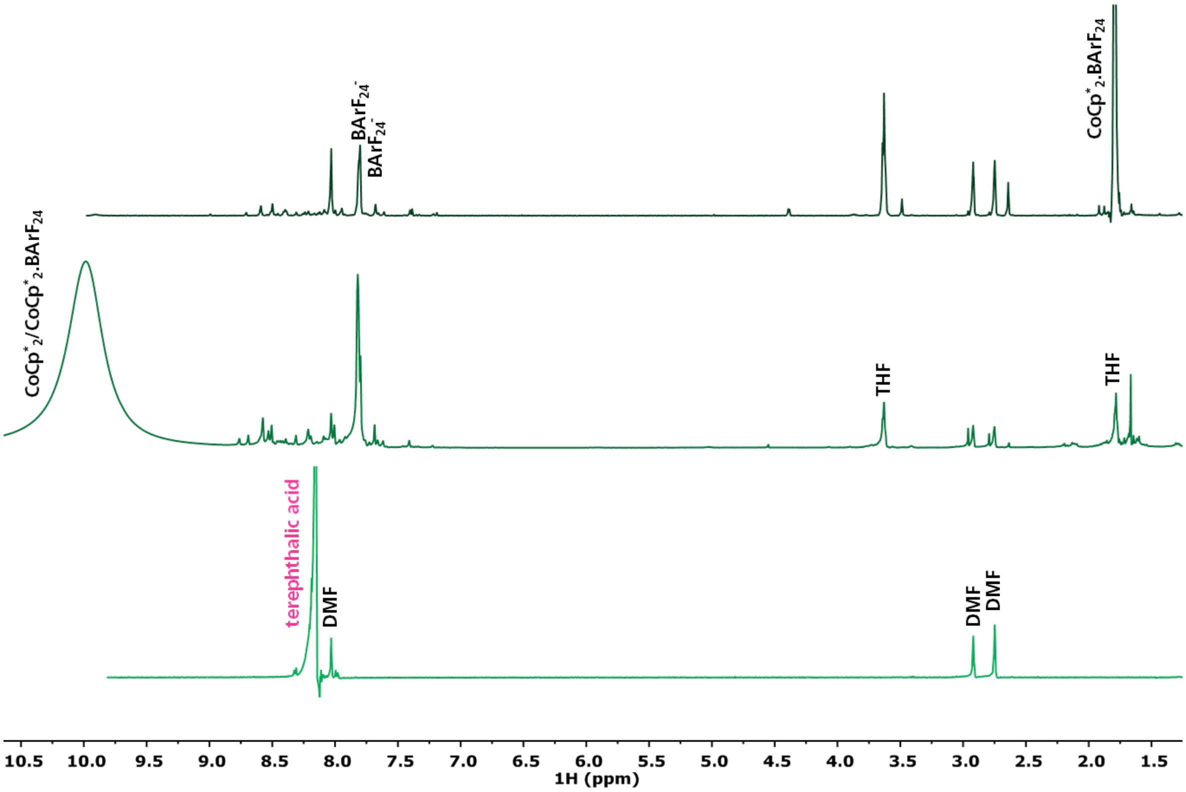

Figure S19. Exemplary ^{1}H NMR (500 MHz, d_7-DMF) spectra of (top): the reaction of MIL-125 (batch 1) with 2 equiv. of CoCp$^*_2$ and 2 equiv. of NaBArF$_{24}$; (middle): the reaction of MIL-125 (batch 1) with 10 equiv. of CoCp$^*_2$ and 10 equiv. of NaBArF$_{24}$; (bottom): terephthalic acid.

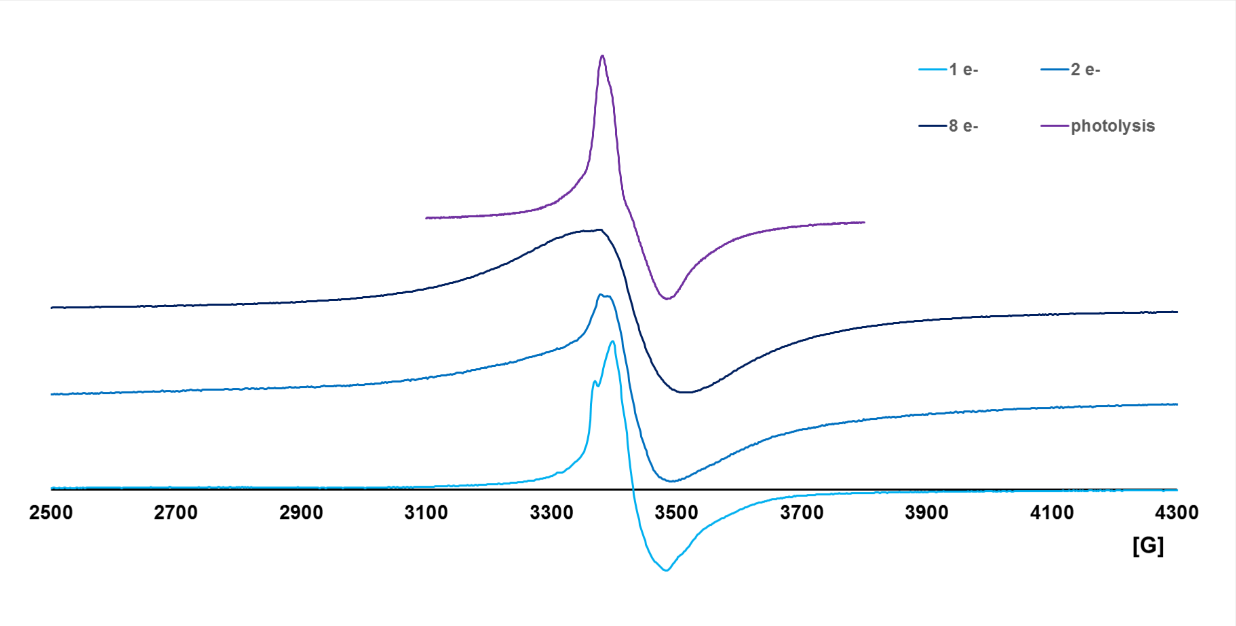

Figure S20. Stacked X-band EPR Spectra of reduced MIL-125. (top, purple): photoreduced MIL-125 (0.25 e^-/H^+); (middle, dark blue): MIL-125 reduced with 10 equiv. of $CoCp^*_2/NaPF_6$; (middle, light blue): reduced with 2 equiv. of $CoCp^*_2/NaPF_6$; (bottom, sky blue): MIL-125 reduced with 1 equiv. of $CoCp^*_2/NaPF_6$;

H.2.Reduction with $CrCp^*_2$

Stock Solutions Preparations.

Solution A. d_8-THF and d_3-MeCN (4:1 v/v).

Solution B. 0.10 M Tol_2O in solution A.

Solution C. 0.20 M NaTFSI in solution A.

Solution D. 0.20 M [2.2.2]-cryptand in solution A.

Reaction of NH_2-MIL-125, 3 equiv. of Cp^*_2Cr and 0~1 equiv. of NaTFSI. In the glovebox, $CrCp^*_2$ (~9.7 mg, ~0.03 mmol) was loaded in the J. Young NMR tube (5 mm). If $CrCp^*_2$ crystals were sticking to the top of NMR tube, a static gun and a glass pipette were used to blow the crystals down to the tube. Internal standard Tol_2O (0.100 mL solution B, 0.0100 mmol) and solution A (0.1 × 4 mL) were then added into this tube to dissolve $CrCp^*_2$. After a ^1H NMR measurement for the determination of the initial amount of $CrCp^*_2$, the sample was brought back into the box. To this NMR tube was loaded with MIL-125 (15.6 mg, 0.010 mmol) (or NH_2-MIL-125 (16.5 mg, 0.010 mmol)) and a tiny stirring bar (8 mm × 1.5 mm). After the suspension of MOFs was stirred for 15~24 h, the stirring bar was then removed and a custom-designed NMR centrifuge was used prior to data collection to enhance the quality of ^1H NMR spectrum. In a typical NaTFSI titration, five 10 µL aliquots of solution C (0.0020 mmol) were added to the NMR tube, followed by stirring for 15~24 h, removal of a stirring bar, centrifuging, and ^1H NMR collection.

Reaction of NH_2-MIL-125, 3 equiv. of $CrCp^*_2$, 1 equiv. of NaTFSI and 0~1 equiv. of [2.2.2]-cryptand. In the glovebox, $CrCp^*_2$ (~9.7 mg, ~0.03 mmol) and NaTFSI (50 µL solution C, 0.0100 mmol) and internal standard Tol_2O (0.100 mL solution B, 0.0100 mmol) were loaded in the J. Young NMR tube (5 mm), followed by the addition of solution A (0.35 mL). After a ^1H NMR measurement, the sample was brought back into the box. MIL-125 (15.6 mg, 0.010 mmol) (or NH_2-MIL-125 (16.5 mg, 0.010 mmol)) was added to this NMR tube equipped with a tiny stirring bar (8 mm × 1.5 mm). After the suspension of MOFs was stirred for 15~24 h, removal of a stirring bar and centrifuging, ^1H NMR spectrum was collected again. In a typical [2.2.2]-cryptand titration, five 10 µL aliquots of solution D (0.0020 mmol) were added to the NMR tube, followed by stirring for 15~24 h, removal of a stirring bar, centrifuging, and ^1H NMR collection.

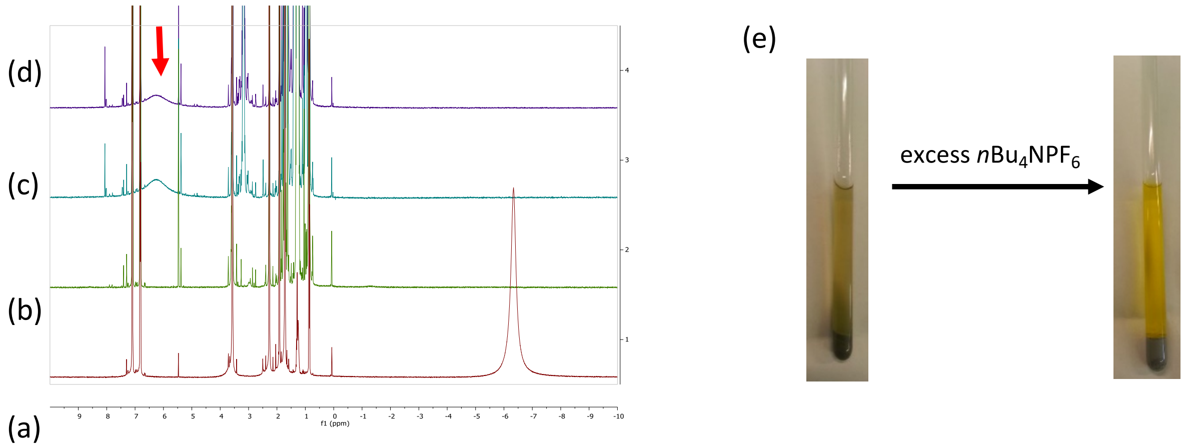

Figure S21. (a)-(d) ^1H NMR spectra showing $CrCp^*_2{}^+$ (red arrow) is attached on the surface of charged MIL-125 after the reaction of $CrCp^*_2$ and MIL-125 (0.005 mmol $(p\text{-tolyl})_2O$ as an internal standard). (a) 0.0025 mmol $CrCp^*_2$ [d_8-THF and d_3-MeCN (4:1 v/v)]. (b) Addition of 0.030 mmol MIL-125 to sample (a). (c) Addition of 0.025 mmol nBu_4NPF_6 into sample (b). (d) Addition of 0.025 mmol $[nBu_4N]PF_6$ into sample (c). (e) Solution color change of reactions (b) and (d).

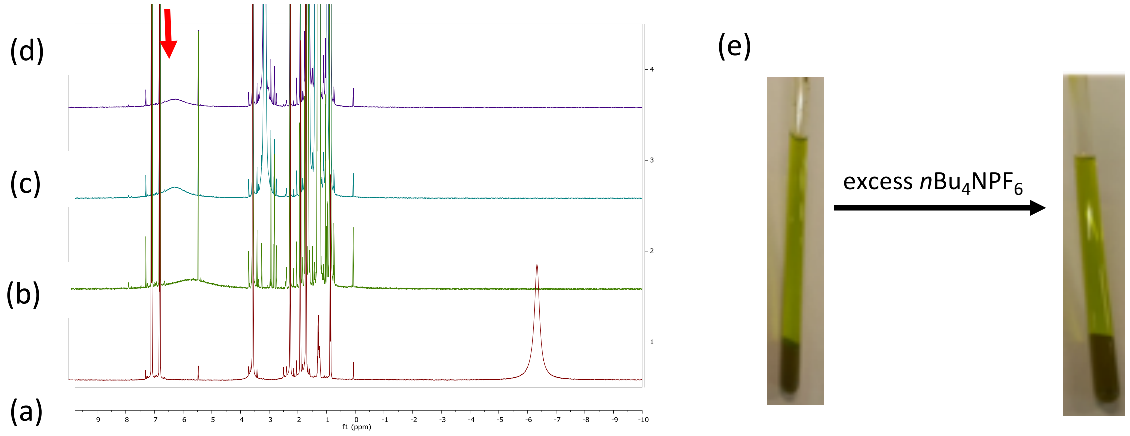

Figure S22. (a)-(d) ^{1}H NMR spectra showing $CrCp^*{}_2{}^+$ (red arrow) is attached on the surface of charged NH_2-MIL-125 after the reaction of $CrCp^*{}_2$ and NH_2-MIL-125 (0.005 mmol (*p*-tolyl)$_2$O as an internal standard). (a) 0.0025 mmol $CrCp^*{}_2$ [d_8-THF and d_3-MeCN (4:1 v/v)]. (b) Addition of 0.030 mmol NH_2-MIL-125 to sample (a). (c) Addition of 0.025 mmol *n*Bu$_4$NPF$_6$ into sample (b). (d) Addition of 0.025 mmol *n*Bu$_4$NPF$_6$ into sample (c). Addition of 0 equiv., 10 equiv. and 20 equiv. of *n*Bu$_4$NPF$_6$ into the mixture led to the liberation of 28.2 %, 45.3 % and 48.0 % of $CrCp^*{}_2{}^+$, respectively. (e) Solution color change of reactions (b) and (d). The green color is attributed to the suspension of very small particles of charged NH_2-MIL-125.

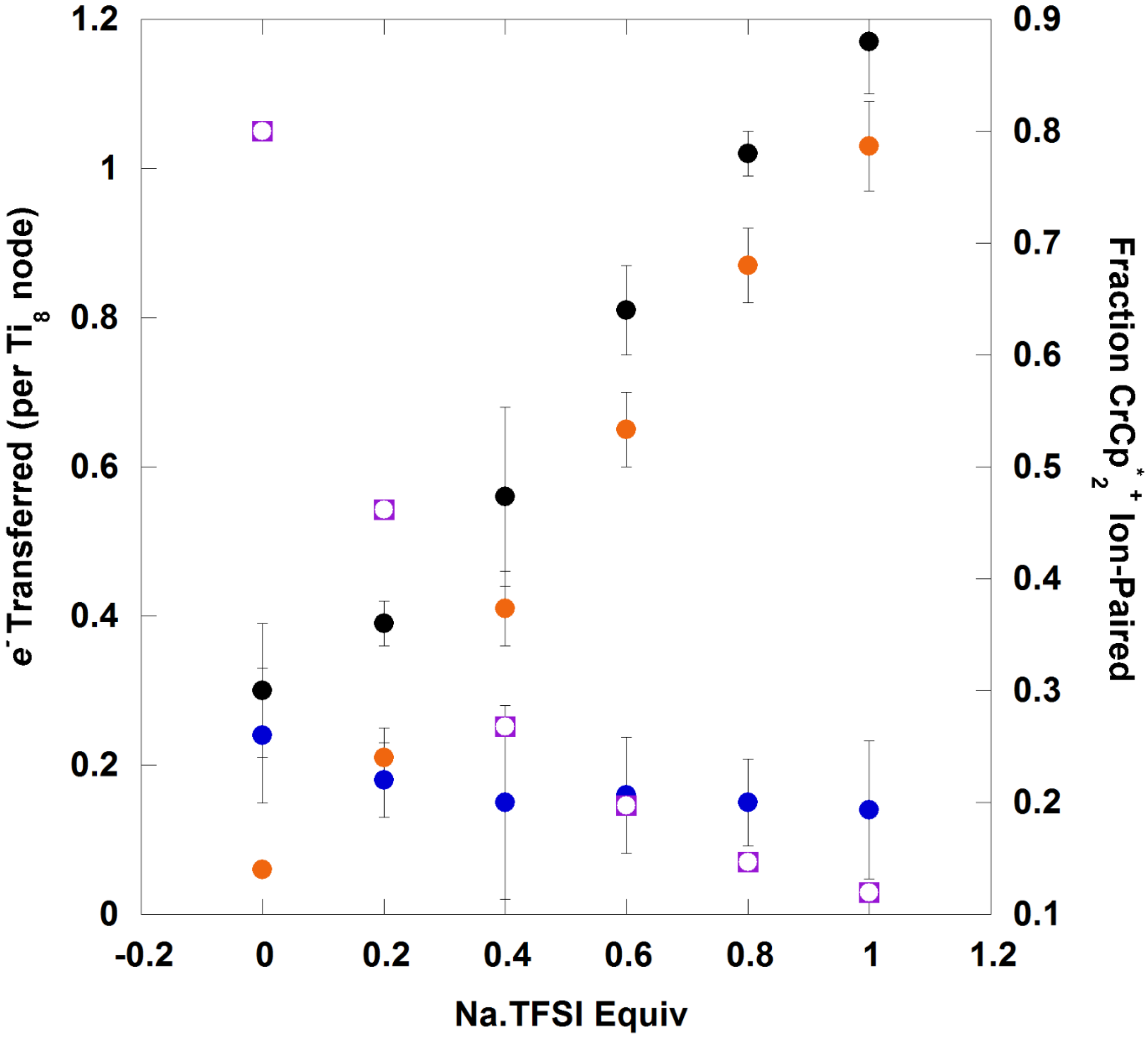

Figure S23. Plot of *e*⁻ transferred to NH_2-MIL-125 (left axis) and fraction of $CrCp^*_2$ ion-paired in reduced NH_2-MIL-125 (right axis) versus equivalents of NaTFSI added. Orange circles represent the equivalents of Na^+ that are associated with the reduced NH_2-MIL-125, derived from the $CrCp^*_2{}^{0/+}$ chemical shift. Blue circles represent the equivalents of $CrCp^*_2{}^+$ that are associated with the reduced NH_2-MIL-125, derived from the change in integration of the $CrCp^*_2{}^{0/+}$ resonance upon mixing with NH_2-MIL-125. Black circles represent the total extent of reduction, and correspond to the sum of the blue and orange circles. Purple squares around white circles represent the fraction of the reduced NH_2-MIL-125 that is associated with $CrCp^*_2{}^+$.

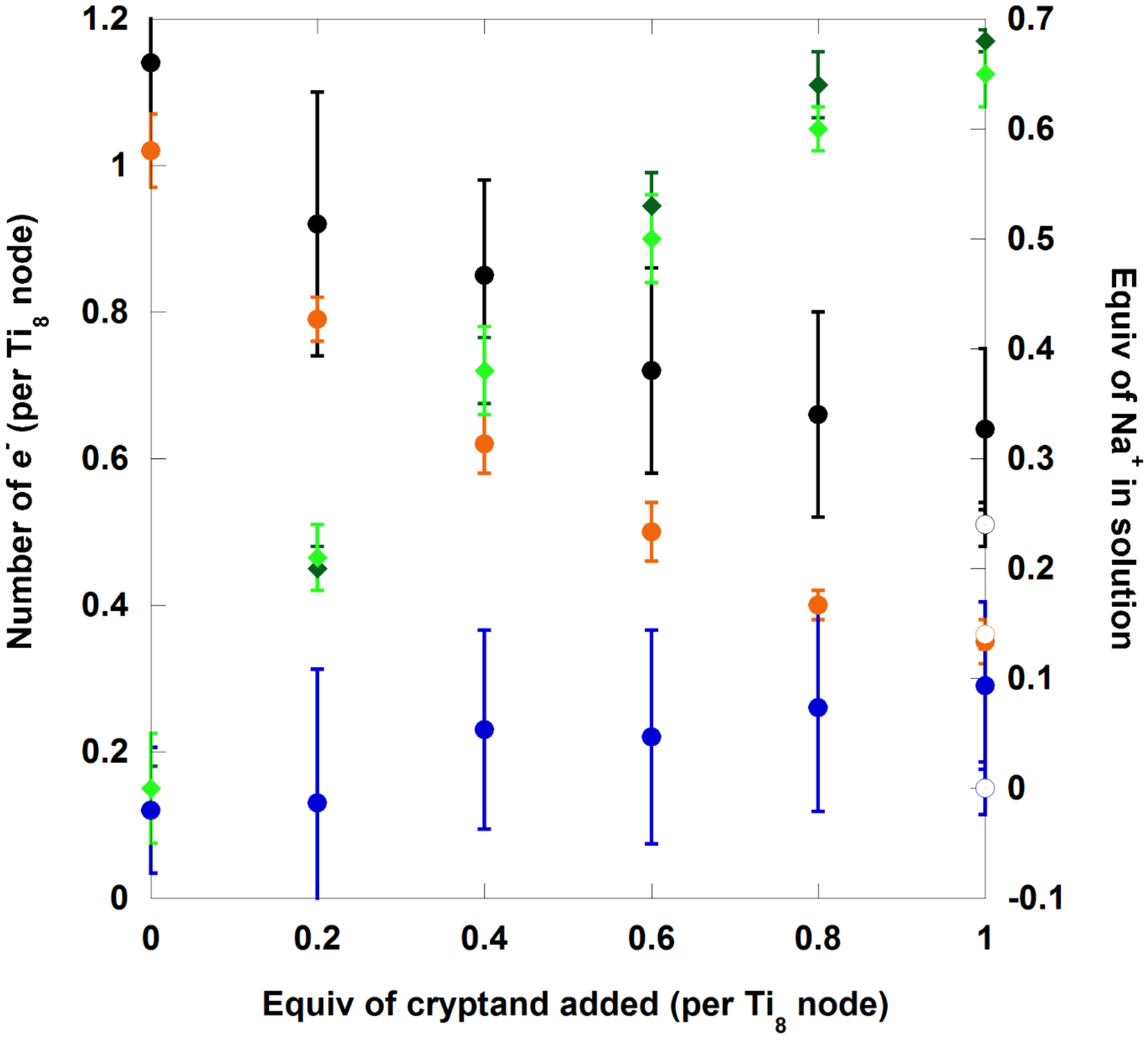

Figure S24. Plot of e^- in NH_2-MIL-125 versus equivalents of cryptand added (left axis), and equiv. of Na^+ in solution (right axis). Orange circles represent the equivalents of Na^+ that are associated with the reduced NH_2-MIL-125, derived from the $CrCp^*_2{}^{0/+}$ chemical shift. Blue circles represent the equivalents of $CrCp^*_2{}^+$ that are associated with the reduced NH_2-MIL-125, derived from the change in integration of the $CrCp^*_2{}^{0/+}$ resonance upon mixing with NH_2-MIL-125. Black circles represent the total extent of reduction, and correspond to the sum of the blue and orange circles. Light green diamonds represent the equiv. of Na^+ in solution, derived from the amount of Na^+ still associated with reduced NH_2-MIL-125. Dark green diamonds correspond to the equiv. of Na^+ in solution, from integration of the cryptand/cryptand-sodium resonances. Unshaded circles correspond to the number of e^- in NH_2-MIL-125 (per Ti_8 node) for the converse reaction: addition of 3 equiv. of $CrCp^*_2$ and 1 equiv. of Na^+(cryptand).

I. ICP-OES Analysis

Inductively-coupled plasma optical-emission spectroscopy (ICP-OES) was carried out using a Perkin Elmer Optima 8300. The standards used were Fluka TraceCert® Ti standard (1000 mg/L Ti in 2% HNO_3) and Fluka TraceCert® multielement standard solution 1 for ICP as the Na standard (50 mg/L Na in 10% HNO_3). Samples were added to Falcon tubes using a plastic spatula and digested with 5 mL of EMD OmniTrace® HNO_3. The concentration of Ti and Na in each sample was determined by the method of standard additions. Each of the samples contained a 100 µL aliquot of the 5 mL stock solution and 0, 20, 100, and 300 µL of Ti standard or 0, 20, 100, and 500 µL of Na standard, and were diluted with 18 MΩ/cm water to a final volume of 10 mL. Reported values are averages of triplicate runs. A blank with no added sample was treated in the same way and run alongside the other samples. The error in the Na/Ti ratios were propagated from the individual errors in [Na] and [Ti]. Errors from the ICP instrument were negligible (<1%), the more significant error is from glassware/handling, and is calculated from the control sample F. In terms of Na/Ti ratio, the error was ± 0.03 or less in each case.

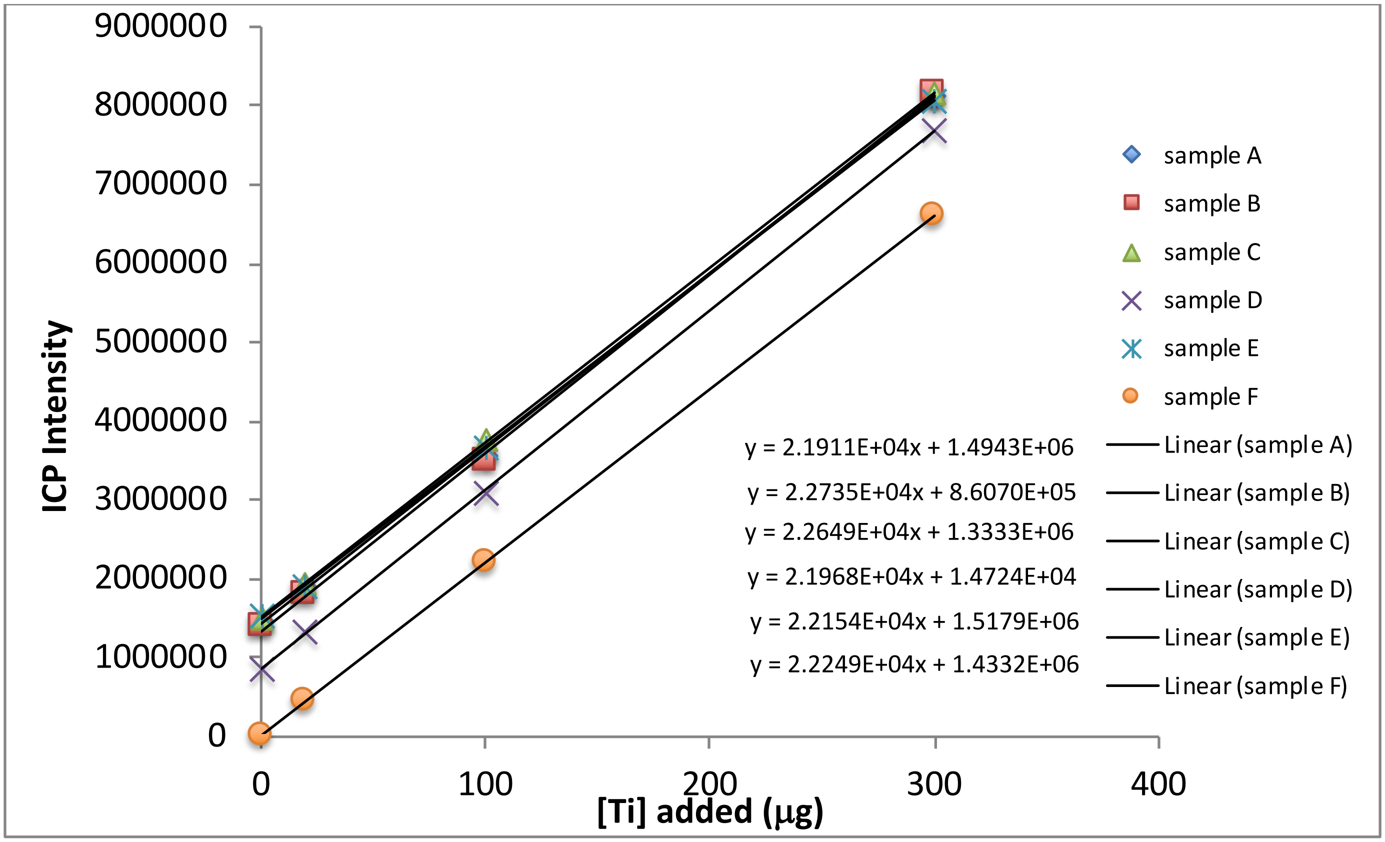

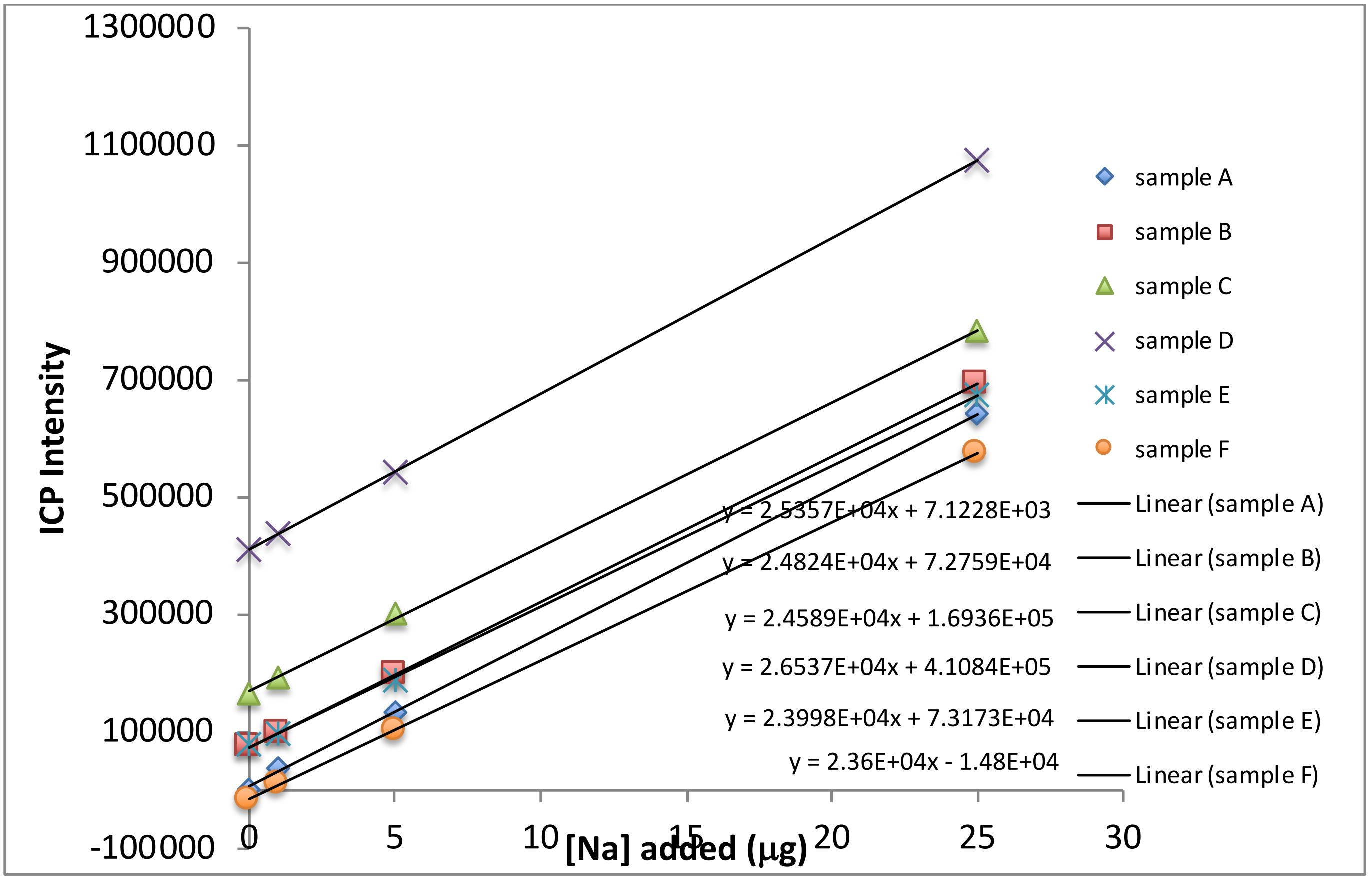

Figure S25. Standard addition method to determine the concentration of Ti or Na in several samples, A is MIL-125 without any added Na, B−E are reduced with $CoCp^*_2$ in the presence of $NaPF_6$ (1, 2, 10, and 1 equiv., respectively), and F is the blank. (top): [Ti] with μg of Ti added on the horizontal axis; (bottom): [Na] with μg of Na added on the horizontal axis.

Table S7. Calculation of Na/Ti ratio in each sample, and the anticipated ratio for comparison. Sample F is the control experiment.

Sample	Found [Na] (mM)	Found [Ti] (mM)	Found Na/Ti ratio	Anticipated Na/Ti ratio
A (batch 2)	0.01	13.5	0.01 ± 0.02	0.00
B (batch 4)	0.1	12.3	0.10 ± 0.03	0.13
C (batch 4)	3.0	14.3	0.21 ± 0.02	0.25
D (batch 2)	6.7	7.9	0.85 ± 0.02	1.00
E (batch 2)	1.3	14.2	0.09 ± 0.03	0.13
F	0.2	0.1	-	-

References

1. A. B. Pangborn, M. A. Giardello, R. H. Grubbs, R. K. Rosen and F. J. Timmers, *Organometallics*, 1996, **15**, 1518-1520.

2. W. L. F. Armarego and C. L. L. Chai, *Purification of Laboratory Chemicals*, Butterworth-Heinmann, London, 2002.

3. V. W. Manner, T. F. Markle, J. H. Freudenthal, J. P. Roth and J. M. Mayer, *Chem. Commun.*, 2008, 256-258.

4. I. J. Rhile, T. F. Markle, H. Nagao, A. G. DiPasquale, O. P. Lam, M. A. Lockwood, K. Rotter and J. M. Mayer, *J. Am. Chem. Soc.*, 2006, **128**, 6075-6088.

5. I. Chávez, A. Alvarez-Carena, E. Molins*, A. Roig, W. Maniukiewicz, A. Arancibia, V. Arancibia, H. Brand and J. Manuel Manríquez*, *J. Organomet. Chem.*, 2000, **601**, 126-132.

6. T. Rodima, V. Maemets and I. Koppel, *J. Chem. Soc., Perkin Trans. 1*, 2000, 2637-2644.

7. F. Neese, *QCPE Bull.*, 1995, **15**, 5.

8. M. Dan-Hardi, C. Serre, T. Frot, L. Rozes, G. Maurin, C. Sanchez, G. Férey and G. Maurín, *J. Am. Chem. Soc.*, 2009, **131**, 10857–10859.

9. Y. Fu, D. Sun, Y. Chen, R. Huang, Z. Ding, X. Fu and Z. Li, *Angew. Chemie - Int. Ed.*, 2012, **51**, 3364–3367.

10. T. Frot, S. Cochet, G. Laurent, C. Sassoye, M. Popall, C. Sanchez and L. Rozes, *Eur. J. Inorg. Chem.*, 2010, **8**, 5650–5659.

11. C. T. Saouma, S. Richard, S. Smolders, R. Ameloot, F. Vermoortele, D. E. De Vos and J. M. Mayer, submitted.